



AFRL-RX-WP-TR-2009-4027

**EVALUATION OF THE StressWave COLD WORKING
(SWCW) PROCESS ON HIGH-STRENGTH ALUMINUM
ALLOYS FOR AEROSPACE**

Eric T. Easterbrook and Michael A. Landy

StressWave, Inc.

FEBRUARY 2009

Final Report

THIS IS A SMALL BUSINESS INNOVATION RESEARCH (SBIR) PHASE II REPORT.

Approved for public release; distribution is unlimited.

See additional restrictions described on inside pages

**AIR FORCE RESEARCH LABORATORY
MATERIALS AND MANUFACTURING DIRECTORATE
WRIGHT-PATTERSON AIR FORCE BASE, OH 45433-7750
AIR FORCE MATERIEL COMMAND
UNITED STATES AIR FORCE**

NOTICE AND SIGNATURE PAGE

Using Government drawings, specifications, or other data included in this document for any purpose other than Government procurement does not in any way obligate the U.S. Government. The fact that the Government formulated or supplied the drawings, specifications, or other data does not license the holder or any other person or corporation; or convey any rights or permission to manufacture, use, or sell any patented invention that may relate to them.

This report was cleared for public release by the Wright-Patterson Public Affairs Office and is available to the general public, including foreign nationals. Copies may be obtained from the Defense Technical Information Center (DTIC) (<http://www.dtic.mil>).

AFRL-RX-WP-TR-2009-4027 HAS BEEN REVIEWED AND IS APPROVED FOR PUBLICATION IN ACCORDANCE WITH THE ASSIGNED DISTRIBUTION STATEMENT.

//signature//

JOHN J. KLEEK
Project Engineer
Materials Test and Eval Group
Acquisition Systems Support Branch

//signature//

CHARLES E. WAGNER, Chief
Branch Chief
Acquisition Systems Support Branch
System Support Division

//signature//

DANIEL J. McDERMOTT
Deputy Chief
System Support Division
Materials and Manufacturing Directorate

This report is published in the interest of scientific and technical information exchange, and its publication does not constitute the Government's approval or disapproval of its ideas or findings.

*Disseminated copies will show "//signature//" stamped or typed above the signature blocks.

REPORT DOCUMENTATION PAGE				<i>Form Approved</i> OMB No. 0704-0188	
The public reporting burden for this collection of information is estimated to average 1 hour per response, including the time for reviewing instructions, searching existing data sources, gathering and maintaining the data needed, and completing and reviewing the collection of information. Send comments regarding this burden estimate or any other aspect of this collection of information, including suggestions for reducing this burden, to Department of Defense, Washington Headquarters Services, Directorate for Information Operations and Reports (0704-0188), 1215 Jefferson Davis Highway, Suite 1204, Arlington, VA 22202-4302. Respondents should be aware that notwithstanding any other provision of law, no person shall be subject to any penalty for failing to comply with a collection of information if it does not display a currently valid OMB control number. PLEASE DO NOT RETURN YOUR FORM TO THE ABOVE ADDRESS.					
1. REPORT DATE (DD-MM-YY) February 2009		2. REPORT TYPE Final		3. DATES COVERED (From - To) 18 August 2006 – 17 December 2008	
4. TITLE AND SUBTITLE EVALUATION OF THE StressWave COLD WORKING (SWCW) PROCESS ON HIGH-STRENGTH ALUMINUM ALLOYS FOR AEROSPACE				5a. CONTRACT NUMBER FA8650-06-C-5606	
				5b. GRANT NUMBER	
				5c. PROGRAM ELEMENT NUMBER 65502F	
6. AUTHOR(S) Eric T. Easterbrook and Michael A. Landy				5d. PROJECT NUMBER 3005	
				5e. TASK NUMBER ML	
				5f. WORK UNIT NUMBER S22T0100	
7. PERFORMING ORGANIZATION NAME(S) AND ADDRESS(ES) StressWave, Inc. 6644 South 196th Street, Suite T-106 Kent, WA 98032				8. PERFORMING ORGANIZATION REPORT NUMBER TR AL20-1	
9. SPONSORING/MONITORING AGENCY NAME(S) AND ADDRESS(ES) Air Force Research Laboratory Materials and Manufacturing Directorate Wright-Patterson Air Force Base, OH 45433-7750 Air Force Materiel Command United States Air Force				10. SPONSORING/MONITORING AGENCY ACRONYM(S) AFRL/RXSC	
				11. SPONSORING/MONITORING AGENCY REPORT NUMBER(S) AFRL-RX-WP-TR-2009-4027	
12. DISTRIBUTION/AVAILABILITY STATEMENT Approved for public release; distribution is unlimited.					
13. SUPPLEMENTARY NOTES This is a Small Business Innovation Research (SBIR) Phase II report. PAO case number: 88ABW-2009-3163; clearance date: 14 July 2009. Letter from contractor waving SBIR data rights on file. Report contains color.					
14. ABSTRACT This report was developed under a SBIR contract. A new and innovative cold working process called StressWave Cold Working (SWCW) was investigated and compared to the conventional split sleeve cold working method that is used to enhance the fatigue life of fastener holes in high strength aluminum alloys used on USAF aircraft structures. StressWave cold working was found to be superior in enhancing fatigue lives compared to split sleeve cold working in both constant amplitude and spectrum fatigue loading environments, when used in its preferred embodiment, upstream cold working. The investigation also included extensive finite element analysis, in the post-yield regime which revealed the presence of deep compressive stresses throughout the thickness of specimens examined. This study also evaluated the fatigue and crack growth performance of over 300 specimens, which demonstrated the superior performance of Upstream StressWave cold working as compared to the split sleeve method. The new method was also shown to be significant less expensive than the split sleeve method for a USAF fighter aircraft program currently under development. Various production implementation methods were investigated and proof-of-concept physical and hardware models were produced.					
15. SUBJECT TERMS SBIR Report, StressWave Cold Working, Split Sleeve Cold Working, High Strength Aluminum Alloys, Fatigue Life Enhancement, Short Transverse Cracking, 70S5 Aluminum, 7050 Aluminum, Spectrum Crack Growth, Compressive Residual ; Stress Finite Element Analysis					
16. SECURITY CLASSIFICATION OF:			17. LIMITATION OF ABSTRACT: SAR	18. NUMBER OF PAGES 64	19a. NAME OF RESPONSIBLE PERSON (Monitor) John J. Kleek 19b. TELEPHONE NUMBER (Include Area Code) (937) 656-6064
a. REPORT Unclassified	b. ABSTRACT Unclassified	c. THIS PAGE Unclassified			

StressWave

6644 South 196th Street, Suite T-106
Kent, WA 98032

253-395-1011 T
253-981-0273 F

May 20, 2009

Mr. John Kleek
Materials Engineer
Air Force Research Laboratory
2179 Twelfth St (AFRL/RXSC)
Wright-Patterson AFB, OH 45433

Subject: USAF/AFRL Report

Dear John:

StressWave, Inc. waives any SBIR data rights with regard to the final report generated from USAF contract FA8650-06-C-5606, and approves the public release of the report.

Best regards,

A handwritten signature in black ink, appearing to read "Michael Landy".

Michael Landy
President

Table of Contents

Section	Page
List of Figures	iv
List of Tables	v
1. Summary	1
2. Introduction	2
3.0 Analysis	5
3.1 Analysis Introduction	5
3.2 Analysis Methodology	5
3.3 Validation of Analysis Methodology	6
3.4 Indenter Design	13
3.5 Finite Element Model Building	15
3.6 Material Models	18
3.7 Hardening Model	19
3.8 Results	20
4.0 Test Program	25
4.1 Test Program Introduction	25
4.2 Specimen Preparation	26
4.3 Fatigue Testing	29
4.3.1 Test Protocol	29
4.3.2 Test Results	30
5. Tooling Development	40
5.1 Tooling Development Introduction	40
5.2 On-Device (End Effector) Tool	40
5.3 Portable (On-Aircraft) Manual Tool	42
5.4 Stand-Alone (Piece Part) Tool	43
6. Conclusions	49
7. Recommendations	51
8. References	52
LIST OF ACRONYMS, ABBREVIATIONS, AND SYMBOLS	54

List of Figures

Figure	Page
Figure 1. StressWave Cold Working (SWCW)	2
Figure 2. Typical SWCW Dimples	2
Figure 3. StressWave Indenter and Corresponding Dimple (for a 1 inch CW hole)	3
Figure 4. Comparison of Residual Stress Distribution, StressWave vs. Split Sleeve	3
Figure 5. 2D Axisymmetric Model with Quarter Symmetry (2DQ)	8
Figure 6. 2D Axisymmetric Model with Half Symmetry (2DH)	8
Figure 7. 3D Full Model (3DF)	9
Figure 8. X-Ray Diffraction Data Compared to FE Analysis Models	9
Figure 9. 2D Half Model	10
Figure 10. 3D Full Model	11
Figure 11. 3D Model – Von Mises Stresses (Expansion)	11
Figure 12. 3D Model – Von-Mises Stresses (Relax)	12
Figure 13. 3D Model – Z-Direction Stresses (Relax)	12
Figure 14. Hoop Stress Path Plot Comparison: Predictions and Measurement	13
Figure 15. 2D StressWave ¼ Mesh Model	15
Figure 16. Pressure Foot Tool Schematic	16
Figure 17. Element Model View – Pressure Foot Tool (1/2 View)	17
Figure 18. Element Model View – Pressure Foot Tool (Full View)	17
Figure 19. Material Model Worksheet	18
Figure 20. Isotropic Hardening vs. Kinematic Hardening	19
Figure 21. Hoop Stress, Maximum Indenter Engagement	20
Figure 22. Resulting Hoop Stress, After Hole Cutting	20
Figure 23. Generic Pocket FE Model	21
Figure 24. Close Up of Indenter (red) and the Mesh Details at the Hole	21
Figure 25. Von-Mises Stresses of the Pocket at Full Indenter Engagement	22
Figure 26. Von Mises Stresses after Hole Trimming and Relax	22
Figure 27. Hoop Stresses on Cut Section after Hole Trimming and Relax (Straight View)	23
Figure 28. Hoop Stresses on Cut Section after Hole Trimming and Relax (Oblique View)	23
Figure 29. Comparison of Residual Stresses, StressWave and Split Sleeve (1.125 Inch Hole) ...	24
Figure 30. Cut diagram for “LT” & “LS” specimen orientations from 7085 & 7050 plate	26
Figure 31. Specimen blanks as cut from plate (a) and prior to cold working (b)	26
Figure 32. Fatigue Specimen Dimensions	27
Figure 33. Typical SWCW Indenting Setup	28
Figure 34. Specimen Dimples (1.125, 0.4375, 0.250)	28
Figure 35. SWCW Specimen Assembly (1.125 inch hole shown)	29
Figure 36. Typical Constant Amplitude Test Setup	29

Figure 37. Constant Amplitude Fatigue Test Results – 7085-T7651 – 0.250 inch –LT Grain Orientation	32
Figure 38. Constant Amplitude Fatigue Test Results – 7085-T7651 – 0.4375 inch –LT Grain Orientation	33
Figure 39. Constant Amplitude Fatigue Test Results – 7085-T7651 – 1.125 inch –LT Grain Orientation	34
Figure 40. Constant Amplitude Fatigue Test Results – 7085-T7651 – 0.250 inch –LS Grain Orientation	35
Figure 41. Constant Amplitude Fatigue Test Results – 7050-T7451 – 0.250 inch –LT Grain Orientation	36
Figure 42. Constant Amplitude Fatigue Test Results – 7050-T7451 – 0.4375 inch –LT Grain Orientation	37
Figure 43. Constant Amplitude Fatigue Test Results – 7050-T7451 – 1.125 inch –LT Grain Orientation	38
Figure 44. Constant Amplitude Fatigue Test Results - 7050-T7451 – 0.250 inch –LS Grain Orientation	39
Figure 45. Early Design End Effector	41
Figure 46. Proof of Concept Hydraulic Pressure Foot End Effector	41
Figure 47. Schematic of Hydraulic Pressure Foot End Effector	42
Figure 48. Portable Manual SWCW Tool.....	42
Figure 49. Concept Sketch – Automated SWCW Tool	45
Figure 50. Process Control (Typical) – Automated SWCW Tool.....	46
Figure 51. Compliance System Mock-up with 1.125 inch Specimen.....	48

List of Tables

Table	Page
Table 1. Constant Amplitude Test Conditions (R = 0.05)	25
Table 2. Minimum Constant Amplitude Fatigue Life Improvement Factors (LIF), Upstream StressWave Cold Working (SWCW) vs. Split Sleeve (SS).....	31
Table 3. Control and Data Tables (Typical) – Automated SWCW Tool.....	47

1. Summary

A new and innovative cold working process called StressWave Cold Working (SWCW) was investigated and compared to the conventional split sleeve cold working method that is used to enhance the fatigue life of fastener holes in high strength aluminum alloys used on USAF aircraft structures. StressWave cold working was found to be superior in enhancing fatigue lives compared to split sleeve cold working in both constant amplitude and spectrum fatigue loading environments, when used in its preferred embodiment, upstream cold working. The investigation also included extensive finite element analysis, in the post-yield regime which revealed the presence of deep compressive stresses throughout the thickness of specimens examined. This study also evaluated the fatigue and crack growth performance of over 300 specimens, which demonstrated the superior performance of Upstream StressWave cold working as compared to the split sleeve method. The new method was also shown to be significant less expensive than the split sleeve method for a USAF fighter aircraft program currently under development. Various production implementation methods were investigated and proof-of-concept physical and hardware models were produced.

2. Introduction

The objective of this program was to develop a new means to facilitate the fatigue enhancement of high strength aluminum alloys in USAF and other aircraft, for new production and repair, cost-effectively, and with greater throughput. In a Phase I SBIR program (Ref. 1), the company was able to better understand the mechanisms that produce cracks at holes in certain high-strength aluminum alloys (2297/2397-T87 and 7050-T7451) when using legacy methods of cold working, and successfully adapted new cold working technology (StressWave cold working, SWCW) with the ability to produce fatigue and crack growth life improvement in holes in these alloys without cracking.

The patented¹ SWCW process improves the fatigue life and endurance limit of holes or other cutouts in metal structure by imparting beneficial residual stresses into the material before hole cutting operations.

SWCW is accomplished using pairs of specialized tools called indenters (Figure 1). The indenters act simultaneously on both sides of the material and are driven to a specified depth into the opposing faces of the material. This action results in temporary, dimensionally consistent features called dimples. Since the dimples typically have smaller diameters than the final hole diameter, they are completely removed when the hole is drilled. Typical dimples are shown in Figure 2. Dimple shape and size are determined by the specific application.

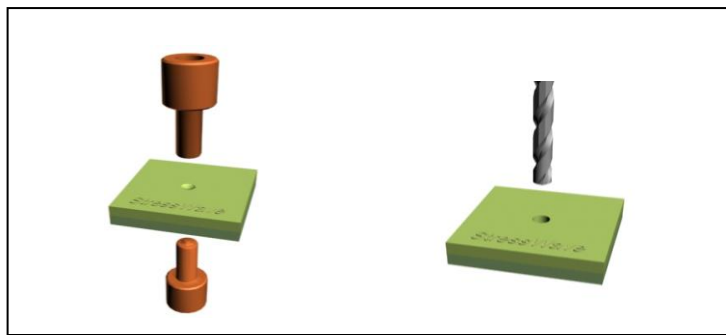


Figure 1. StressWave Cold Working (SWCW)

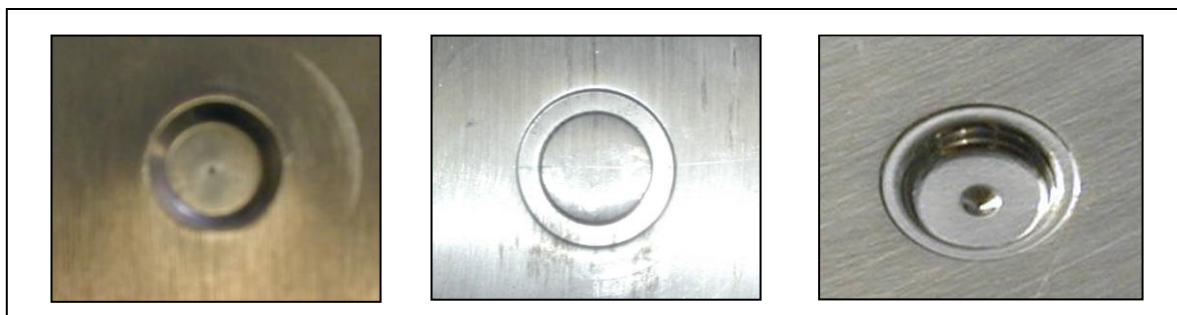


Figure 2. Typical SWCW Dimples

¹ #6,230,537; #6,389,865; #6,615,636; #6,711,928; #6,742,376; #7,024,747; #7,047,786; 7,131,310

SWCW creates a compressive residual stress zone surrounding the hole and through the thickness of the part. One or more surfaces of the material may be milled away to any depth prior to hole drilling with no change to the fatigue life of the SWCW hole. This option, Upstream Cold Working (USCW), can be used to provide distortion free cold worked components (Figure 3).



Figure 3. StressWave Indenter and Corresponding Dimple (for a 1 inch CW hole)

Other independent research and development efforts have also shown that SWCW provides significant life improvement (Ref. 2-11 and others), comparable to legacy mandrel methods of cold working (Figure 4).

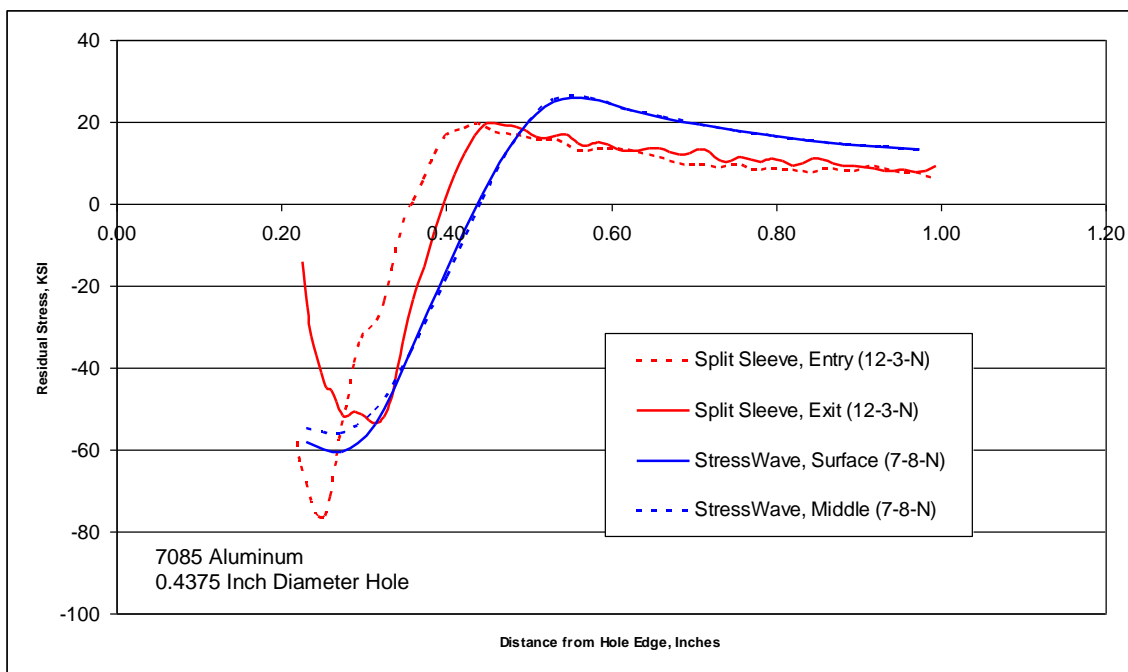


Figure 4. Comparison of Residual Stress Distribution, StressWave vs. Split Sleeve

The key to commercialization of this promising technology requires development of standardized process parameters, manufacturing integration methods, and production tooling concepts. SWCW cold working can be completed early in the production sequence using

USCW, on a piece-part in near net shape condition. The concept of using new technology for cold working piece-parts offers significant opportunities for manufacturing cost reductions. Cold working, currently only done during final assembly, can be moved ahead in the production sequence, even as far as, for example, a forging vendor. Moving cold working upstream lowers production costs by removing expensive manual processing during final assembly.

This Phase II program was designed to help commercialize the technology by the development of a standardized process parameter specification methodology through use of post-yield finite element modeling, design and fabrication of production demonstrator tools, and sufficient fatigue/crack growth testing to ensure process specification accuracy and reliability of manufacturing integration planning guidelines.

Shortly after contract award, a survey trip was taken to Lockheed Martin Aeronautics Corporation (LM). This trip, a planned task as part of the original technical proposal, was taken in order to develop a data base of generic parts (being cold worked or potentially cold worked) that would be used as a basis for the remainder of program tasks. This survey, however, revealed a significant, immediate opportunity within the F-35 program for cost savings on an actual application, penetration holes on wing carry-through bulkheads made from 7085 aluminum. Those parts are currently being cold worked using a legacy method (split sleeve cold working) late in the bulkhead production sequence. With the concurrence of the USAF, it was decided to re-focus the program to be more closely aligned with this actual application. Nonetheless, almost all aspects of the program are applicable to other cold working applications.

It was also decided to add 7050 plate material to the program. This material is also used in F-35 bulkheads and widely used elsewhere in USAF aircraft.

The analysis effort involved exhaustive examination of the behavior of SWCW, and the split sleeve process, using post-yield finite element and optimization methods. That analytical effort provided a basis for standardized selection of process parameters.

Fatigue testing included almost 300 constant amplitude tests at room temperature on two materials, in two different grain directions, three hole sizes, and two stress levels, to provide a basis for S-N curves. During the course of the program, AFRL performed an independent study by performing spectrum crack growth tests on both SWCW and split sleeve cold worked specimens. The specimens were cut from a forging alloy and the specimen design was representative of an F-35 bulkhead penetration hole. The results will be reported separately at a later date.

Tooling development proceeded with initial design work and prototyping for small tools and end effectors, although significant effort was devoted to preliminary design on a large tool for the bulkhead penetration holes. A number of tooling concepts were developed and tested, which can form the basis for many other applications of SWCW.

3.0 Analysis

3.1 Analysis Introduction

The purpose of this task was to establish the optimum SWCW indenter end shapes for the various hole diameters and material thicknesses representing F-35 main bulkheads. Shapes were optimized for the specific aluminum alloys used for making the bulkheads. The optimum end shape ideally induces a zone of residual compressive stresses similar in magnitude and extent as those provided by split sleeve or split mandrel cold working. Several other optimization parameters include uniformity of the residual stresses through the thickness, least amount of process force and ability to process in an upstream fashion.

Two types of indenters are being modeled and evaluated in the optimization task. These are the standard “bullet-shaped” indenters generally used on holes ranging from 3/16 to 1 inch diameter. The other shape, used for the large, F-35 bulkhead penetration holes is cup-shaped. The cup shape reduces process force while applying compressive residual stress at the periphery of the hole.

3.2 Analysis Methodology

The primary software used for this task are LS-Dyna, LS-PrePost and LS-OPT (LSTC, Livermore, California). LS-DYNA is a general purpose transient dynamic finite element program capable of simulating complex problems including non-linear material behavior such as cold working. LS-PrePost is an advanced interactive program for preparing input data for LS-DYNA as well as for processing the results from LS-DYNA analyses. LS-OPT is a standalone design optimization and probabilistic analysis package that interfaces with LS-DYNA. An advantage of LS-Dyna over conventional finite element codes is that it runs in both/either implicit and explicit mode. The explicit mode allows the solution of the StressWave application to be solved many times faster than the implicit mode; a great advantage for the optimizing process where many consecutive different runs need to be made.

In a typical SWCW process analysis using LS-Dyna the problem is generally broken down into three distinct phases; indentation, relax, trim and relax. The indentation phase is the application of the indenter(s) until they reach the prescribed depth into the material. The relax phase removes the indenter from the model and allows the material to springback without the application of external forces. The trim and relax phase is used to “cut” the hole or “machine” any other features followed by a natural material springback as a result of removing the material. This method produces an accurate solution by taking into account the action of the material during and after the indentation as well as the hole drilling and milling operations. Running these separate phases generally requires a restart of the LS-Dyna program after the end of each phase. The restart capability of the program is a powerful tool for analyzing a series of metal forming and other operations.

LS-OPT was used for the optimization routines. Optimization can generally be considered as a procedure that achieves the best outcome of a certain design subject to certain restrictions. In the conventional approach to improving a given design, the design is improved by evaluating its response to certain design changes. Experience, intuition and common sense are usually the best guides for making design changes in the conventional way. Unfortunately, this approach does

not always produce the “best” design as some design objectives may be in conflict. The LS-OPT program uses the inverse of the conventional design approach by first specifying the objectives of the design and then computing the “best” design. This procedure by which design criteria are first incorporated as objectives and constraints into an optimization problem that is then solved for the “best” design is referred to as optimal design. In optimizing the StressWave indenter end shape, the objectives of high compressive residual stress, low residual tensile stress and low applied process force are first set up in the design space. The finite element model has sufficient flexibility to search out a variety of end shapes that provides the “best” outcome.

LS-PrePost is a companion program to LS-Dyna that allows one to pre-process models and post process the results of running the models. The program has capability to perform just about any operation, model view, section cuts and the like necessary to fully evaluate a solution.

3.3 Validation of Analysis Methodology

SW’s predictive capability is based upon use of finite element modeling and analysis, typically in the post-yield regime. Confident use of this model requires validation of the predictive capability.

SW’s methods and practices for finite element analysis of cold working processes, including material models and contact surface simulation, coefficients of friction and model types and element selection and size, provide good correlation to the measured data in the reports selected. In general, 3D models provide better results than 2D models and should be used where necessary for accurate prediction of stresses. 2D quarter finite element models appear to have an inherent stiffness that over predicts both compressive and tensile stress magnitudes and therefore should be avoided.

The validation process involved comparisons to other finite element analyses, X-ray, neutron diffraction data. To further validate the modeling techniques, comparisons were performed against measurements of stresses in specimens cold worked using methods other than StressWave, to determine whether the material and contact models, methods, practices, coefficients of friction and model types provided good correlation. Data sets were selected from published data sets that had low data scatter and enough description of the setup that allowed for accurate re-creation with the SW modeling system.

One of these data sets was an internal report commissioned by SW and performed by Lambda Research in 2001. This study measured the residual hoop stresses from SWCW in a 2.3 x 2.3 x .375 inch thick plate of 4340 steel (R_c 36-40). The faces were stress-free ground to smooth the surface and to remove any potential residual stresses from the milling or heat treating. The top and bottom faces of the specimen were then SWCW with a 360M indenter pair. The measurements were taken at the edge of the hole radially out to the edge of the plate.

The other data set selected was from a study performed by Dietrich and Potter (Ref. 12). The specimens in this study were made from fine-grained 1045 steel that allowed for accurate x-ray diffraction measurements with minimal scatter. The type of cold working was somewhat unconventional in that it was a solid mandrel cold working (no sleeve) where the hole was cold worked to very high strain levels. The 8.1% applied expansion resulted in a permanent hole expansion of 6.2%. The very high expansion level with out-of-plane distortion due to plate

bending was thought to be a good candidate for validating StressWave analysis methods and practices because of the high degree of non-linear behavior. The data shows a typical hoop stress distribution except for the very large zone of reverse yielding at the bore of the hole.

Several finite element models were built to simulate the components of the SW/Lambda and Ref. 12 test setups. The indenter shapes, mandrel diameter, starting hole diameter, plate dimensions, boundary conditions, and material property data were known. For the Ref. 12 study, some items had to be assumed about the setup, as they were not noted in the report, but based on experience were estimated to be reasonable and would not result in any substantive differences in results. These included mandrel taper of 0.045 in/in, a 0.060 inch wide flat width on the mandrel major diameter, and the geometry of the nosecap. For the nosecap a hollow cylinder with an outside diameter of .500 inch larger in diameter than the mandrel major diameter and an inside diameter slightly larger than the major mandrel diameter was used.

Several finite element models were built for the SW/Lambda report and are described below in order of complexity with their corresponding model identification –

- 2D axisymmetric model with quarter symmetry (2DQ)
- 2D axisymmetric model with half symmetry (2DH)
- 3D full model (3DF)

In a like manner two finite element models were constructed to simulate the setup in Ref. 12.

- 2D axisymmetric model with half symmetry
- 3D full model

The 2D models were made from four-sided quadrilateral shells and the 3D models built from six-sided brick (hex) elements. The results from each of the runs were compared to the X-ray diffraction measurements. The material model for each of the validation efforts was derived from mechanical property data taken from Ref. 13 and the Ramberg-Osgood equation resulting in a full stress-strain curve. The geometry and element size selection of the model was constructed so that the data is taken at a depth of about 0.010 inch from the surface – about the depth of the x-ray diffraction readings.

A typical run of the 2D models included 3 steps; 1) Cold work, 2) material springback and 3) cut final hole and final springback. The 3D models used only steps 1 and 2. For some of the mandrel cold working analysis runs both entry and exit side data are shown as it is not specified from which side the measurements were taken in the Ref. 12 report.

The FE models for the Lambda report are shown in Figures 5 through 7 with the comparison of data and measurement shown in Figure 8.

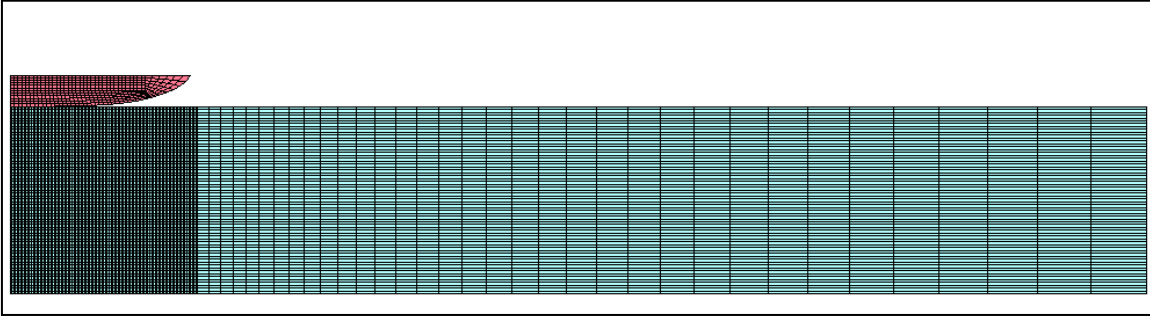


Figure 5. 2D Axisymmetric Model with Quarter Symmetry (2DQ)

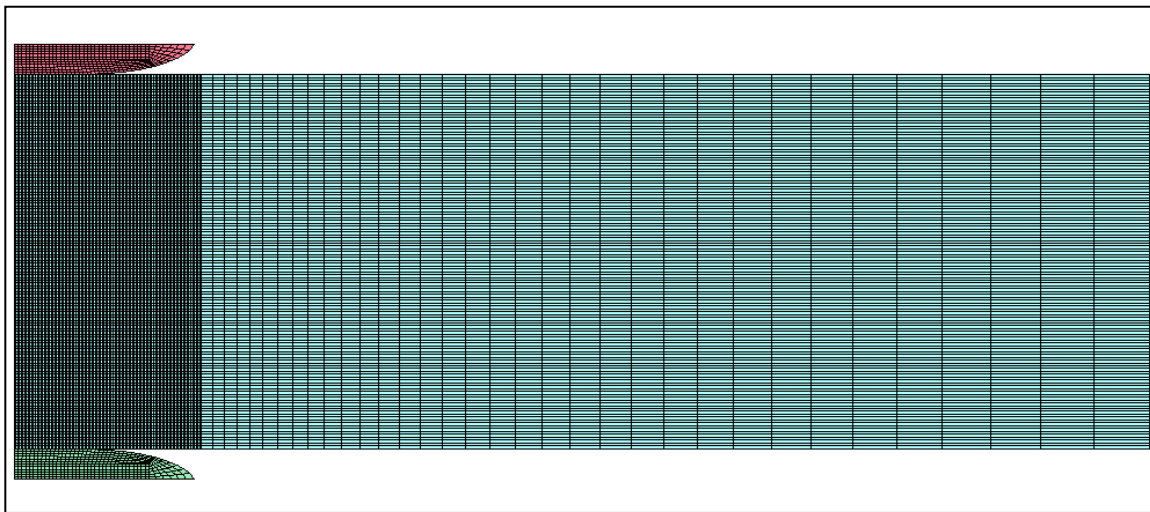


Figure 6. 2D Axisymmetric Model with Half Symmetry (2DH)

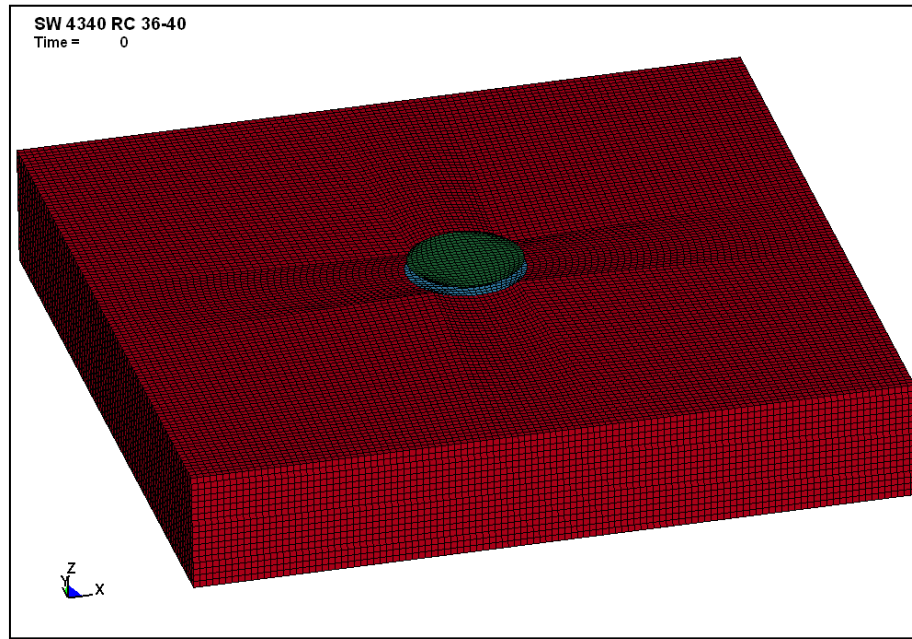


Figure 7. 3D Full Model (3DF)

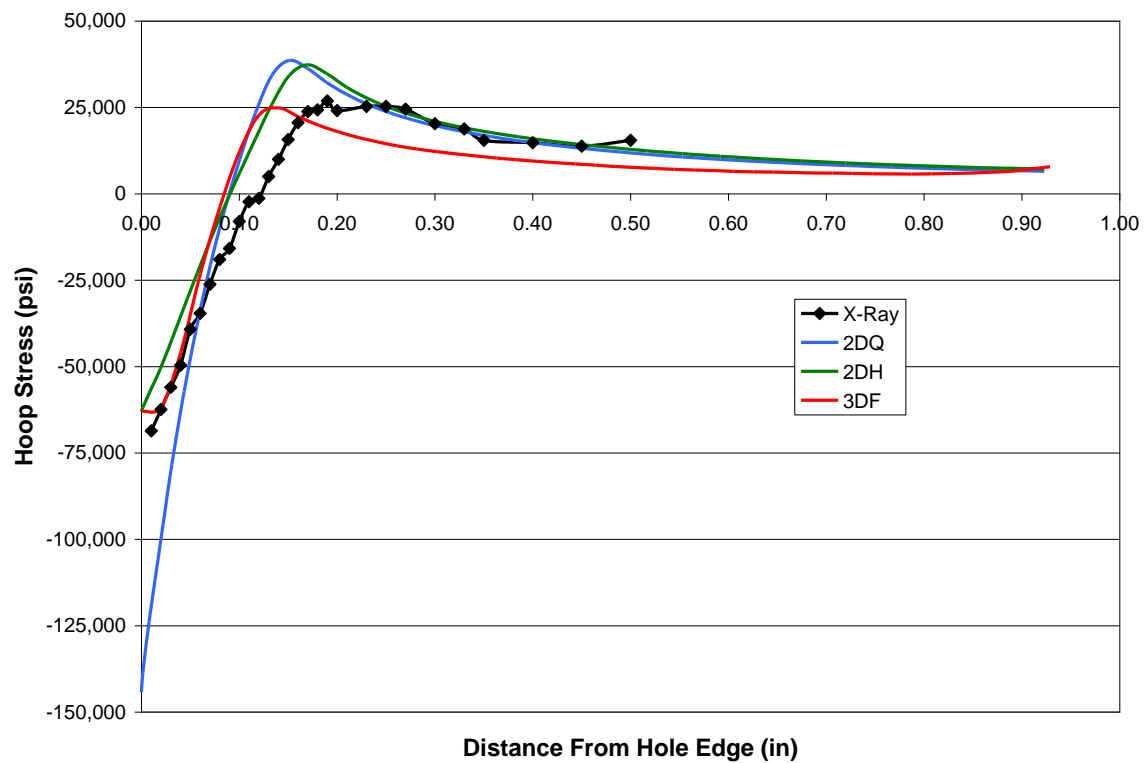


Figure 8. X-Ray Diffraction Data Compared to FE Analysis Models

It is clear that the 2D quarter symmetry model (2DQ) over predicted the magnitudes of both the compressive and tensile stresses. The 2D half symmetry (2DH) well predicted the magnitude of the compressive stress, but over predicted the magnitude of the tensile stresses. The 3D full model well predicted both the magnitudes of the compressive and tensile stress zones. In all cases the extent (radial distance) of the compressive zone was under predicted by about 0.025 inch.

The models for the Ref. 12 study are shown in Figures 9 and 10. Both 2D and 3D models comprises a mandrel (red), test specimen (blue) and nosecone (green). The mandrel was modeled as a rigid body, the plate with 1045 steel properties and the nosecone as steel (elastic). The Von-Mises stresses, just as the mandrel exits, are shown in Figure 11. The rather chaotic pattern of stresses is due to the speed of the simulation using the explicit method of analysis. The same Von-Mises stresses look much more orderly after a natural springback of the material using the implicit method of analysis as shown in Figure 12. The hoop stresses, in this case in the z-direction, are shown in Figure 13. Finally, a comparison of the stresses and measurements is shown in Figure 14.

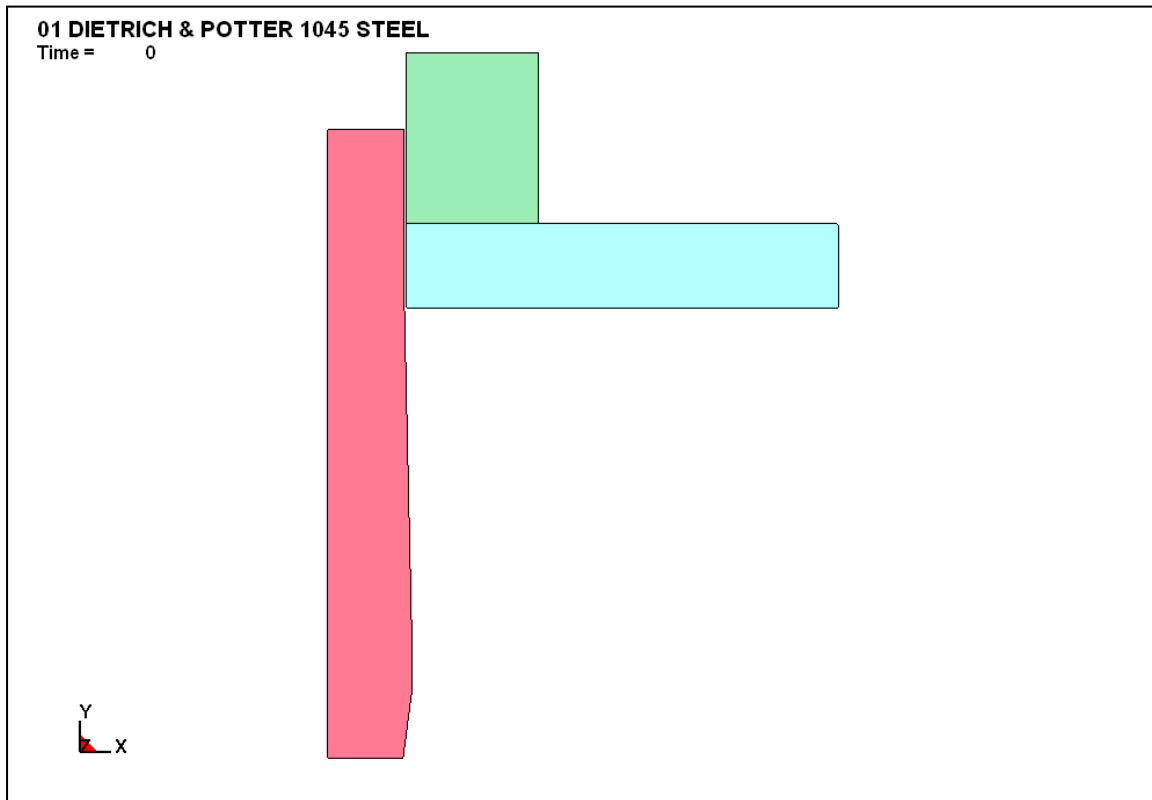


Figure 9. 2D Half Model

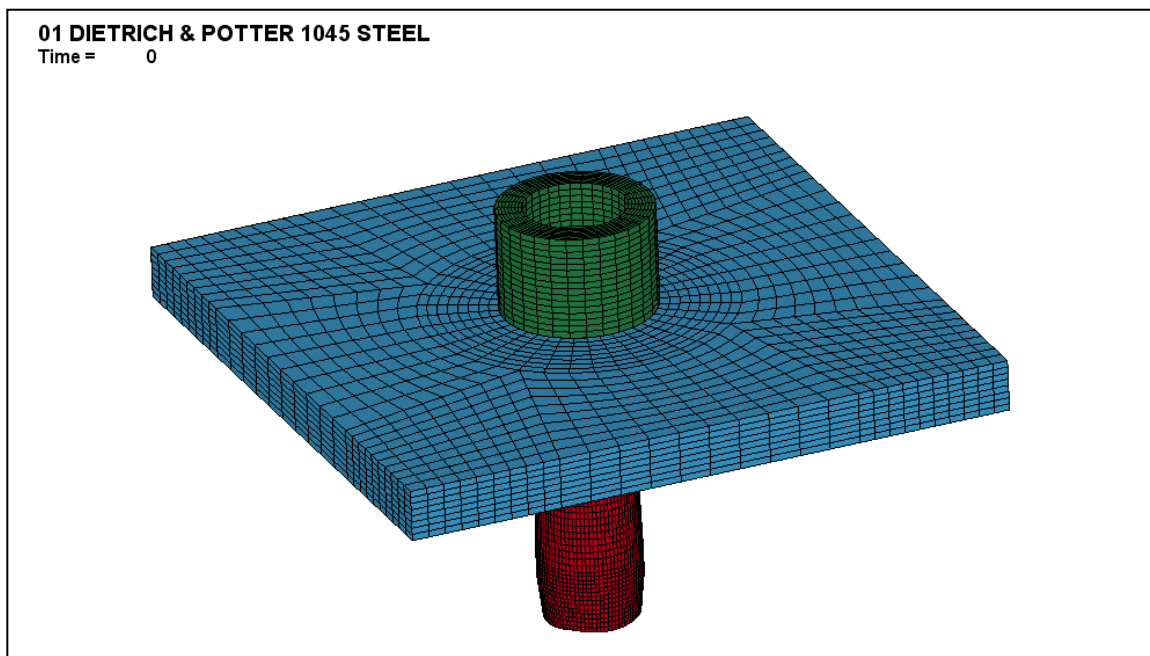


Figure 10. 3D Full Model

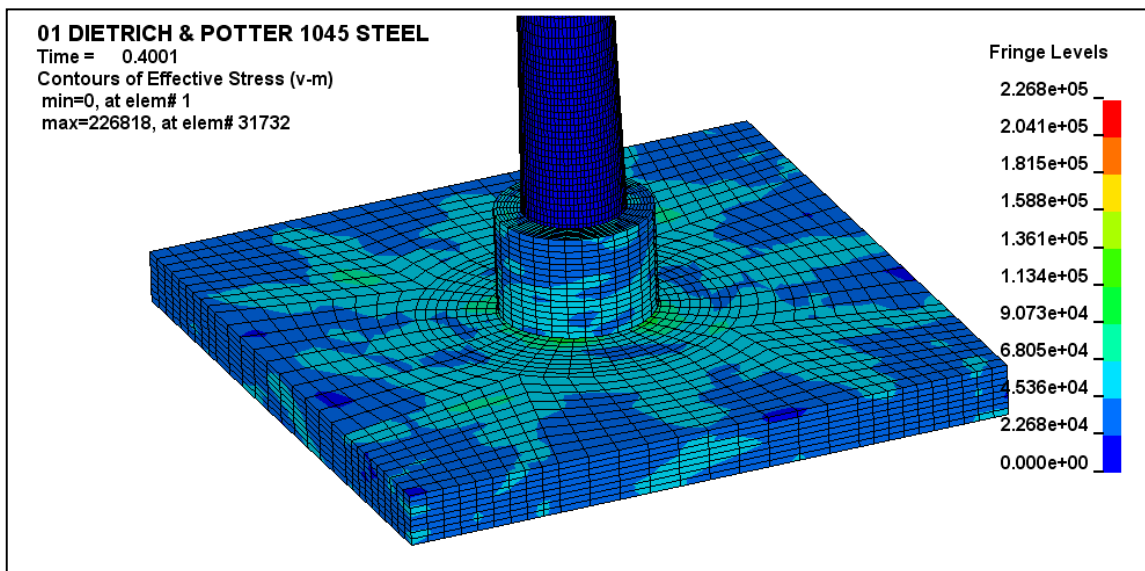


Figure 11. 3D Model – Von Mises Stresses (Expansion)

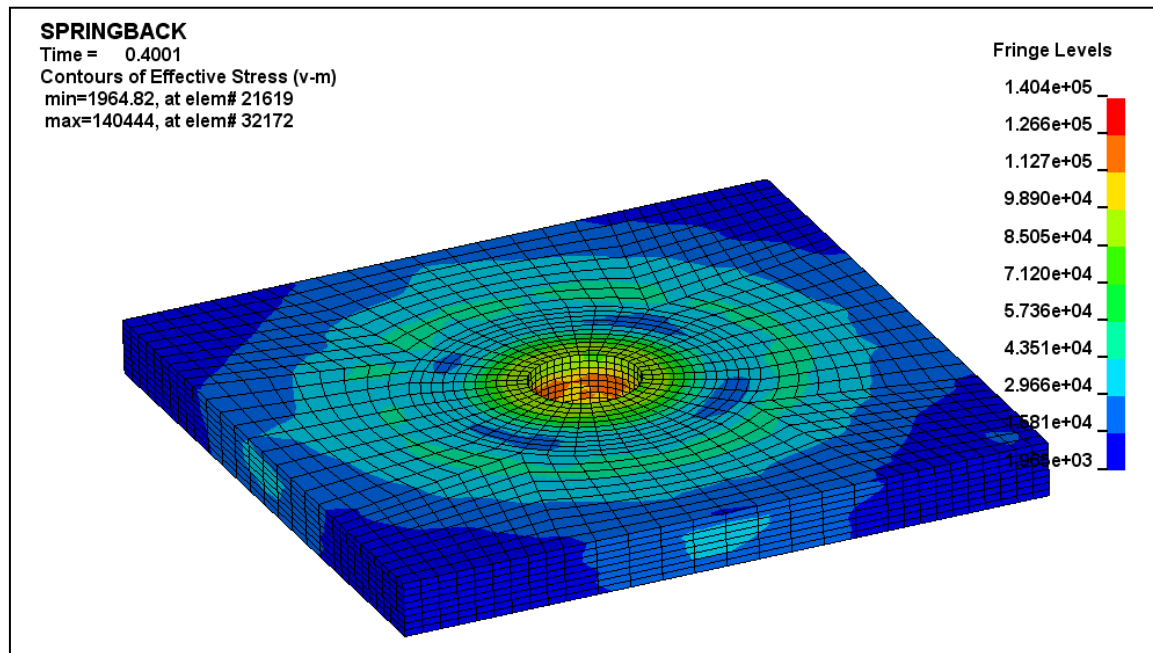


Figure 12. 3D Model – Von-Mises Stresses (Relax)

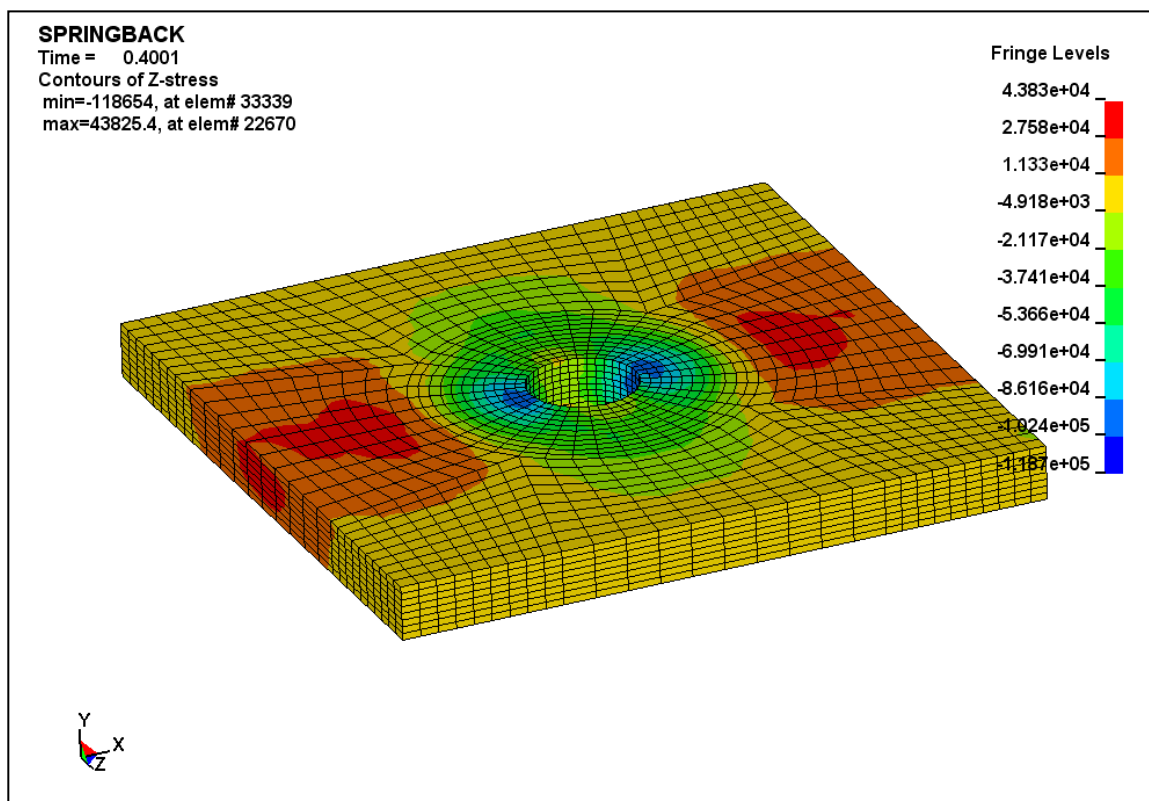


Figure 13. 3D Model – Z-Direction Stresses (Relax)

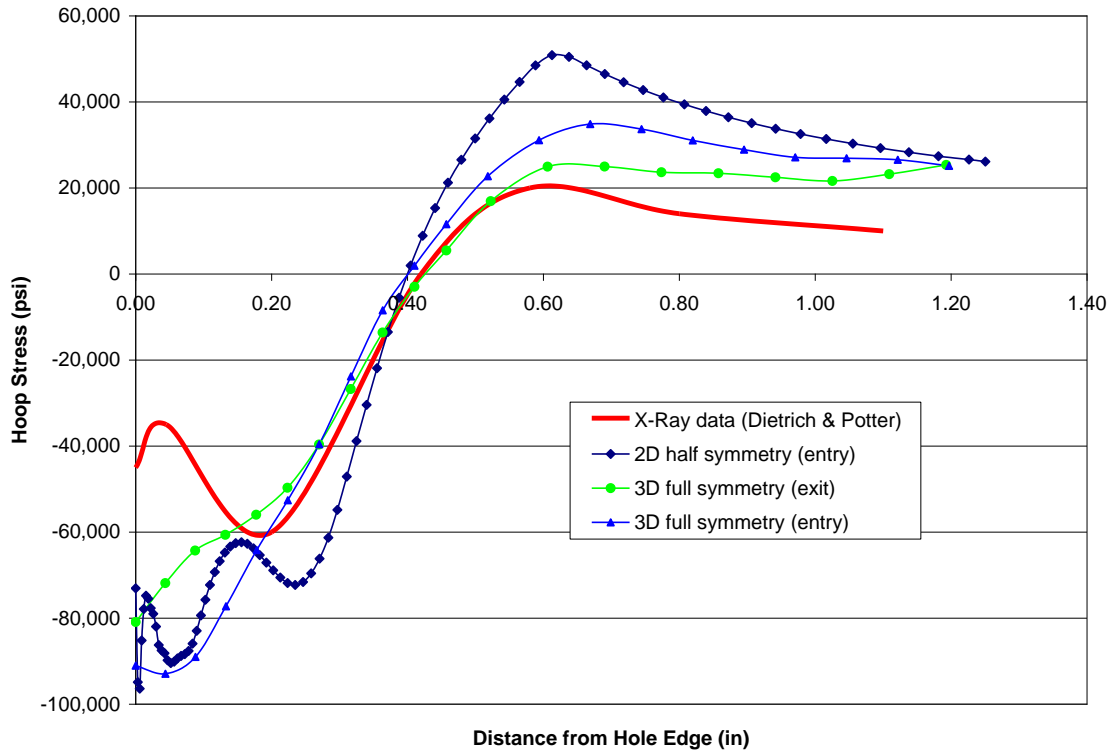


Figure 14. Hoop Stress Path Plot Comparison: Predictions and Measurement

The data shows that the 3D model better predicts the residual stress magnitudes measured using x-ray diffraction. In all cases the zone size of the compressive stresses was well predicted at about 0.400 inches from the edge of the hole. In two cases the effect of re-yielding was evidenced by the reversal(s) in stress magnitude; 2D entry side and 3D entry side. The 2D exit side data is not shown as it had very localized spikes in stress due to distortion and contact.

3.4 Indenter Design

The end shape(s) for the SW indenters have been thoroughly tested in a number of fatigue and crack growth tests. The particular profile of the ‘bullet-shape’ indenter is based on years of analysis and fatigue test experience in both aluminum and titanium materials. Still, an optimization process like the one previously described has not been run (until now) to determine if the shapes could be adjusted to meet the objectives more precisely.

A previous SWCW specification uses an indenter design limited to a particular range of material thicknesses before requiring the use of a different indenter model. This is referred to as the thickness range for a particular indenter model. The current thickness range of indenters designed for holes less than one inch diameter is about 1/8 inch. Using the optimization program it is very likely that the thickness range for a given indenter shape could be increased substantially. Work done in the past has shown that indenter models can work on material thicknesses much wider than the current SW specification thickness range. This effect of increasing the thickness range has the benefit of minimizing the number of indenter shape for a given cold working task.

The optimization of the end shape of the cupped indenters representing F-35 bulkhead penetration holes takes a similar approach, but is more complex because of the increased number of design parameters (about 12 to 14) and the shape of the final part which includes a diametric “boss” around the final hole. The boss limits the extent of material with which the compressive stresses are balanced by a tensile zone. This has the effect of piling up tensile stresses in the web just beyond the boss. Early FE runs of a 2D boss model show that StressWave can be used very effectively in these areas. The optimization process for these areas includes the following steps;

1. A FE model is constructed and the robustness of the model is checked by changing the value a various features to ensure that the FE model does not break down. In certain cases the mesh created by the TrueGrid processor, using the selected limits of design, may not be optimal for the type of contact analysis used.
2. A check is made to ensure that the design variables, dependents and constants are substituted as intended.
3. The limits of the variables are selected so that the model generates properly. This is related to the robustness check in Step 1.
4. Modify the input, if necessary, to define the experiment for a full analysis.
5. Execute LS-OPT and monitor its process.

By following these steps optimized indenter end shapes were calculated. It should be noted that while these steps are easy in concept the work necessary to accomplish them involves changing code by the software supplier.

As good as these programs are for the analysis and optimization of a given process, shape, parameter, etc., LS-OPT has a major limitation for optimizing SWCW directly for compressive residual stress. The reason for this limitation is LS-OPT’s inability to work with restarts². It can currently only analyze a single run. Since one of the key design parameters for optimizing the SWCW is the size and magnitude of the compressive residual stress zone and that is not generally calculated until the 3rd restart (the step when the hole is cut and then relaxed) there is no direct way to optimize on residual stresses. This makes the development of a “transfer function” between the design shape and indentation depth and resulting residual compressive stresses necessary. In this way, the characteristics of what makes for good residual stresses in the trim and relax phase need to be identified in the indentation phase.

A first step to solving the problem includes running the indentation and initial relaxation step in one run using a “seamless springback” command in the keyword file of the LS-Dyna input. This collapses the first two runs into one longer run. A variety of simulations have been run showing the accuracy of combining the first two steps.

²LSSTC recently provided a means to use restarts in LS-OPT by using the concept of cases. The cases are organized in a single file with commands to delineate their beginning and end. This recent capability has provided the means to optimize residual stresses directly. StressWave is using this method for all cold working optimization.

It has been observed that the optimal indenter shape and indentation depth calculated by the limited relaxed residual stresses (indent and seamless springback run) provides for very good residual stresses when the optimized indenter geometry and indentation parameters are inserted into a typical three step solution. For now, this solution method works, but it is very desirable to find a direct solution for residual stresses.

3.5 Finite Element Model Building

The mesh models were developed from the solid models using a commercially available code, TrueGrid® (XYZ Scientific Applications, Livermore, CA). TrueGrid® is a general purpose mesh generation pre-processor with sophisticated relaxation and parameterization capabilities. It has been optimized to produce high quality, structured, multi-block hex meshes or grids and serves as a preprocessor to many analysis codes. TrueGrid is used to pre-process the jobs running in LS-OPT. It quickly forms the mesh using inputs from LS-OPT. LS-OPT then queues the jobs for LS-Dyna.

The basic 2D SW model is axi-symmetric and analyzes the effect of the indenter and material only. The indenters are shown in red and the material in light blue. A thin black line shows the planes of symmetry used for the model. Only a $\frac{1}{4}$ of the model is needed to do the analysis. This simplifies the modeling and reduces solution time. Mesh details of a portion of the $\frac{1}{4}$ model are shown in Figure 15.

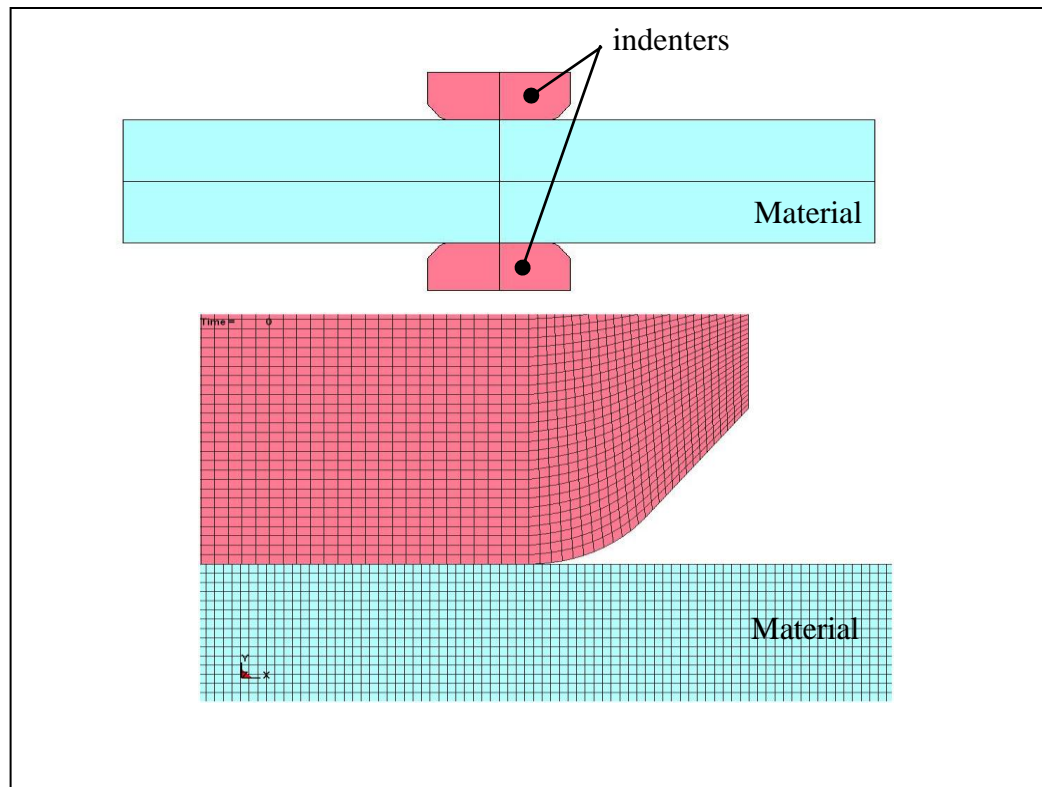


Figure 15. 2D StressWave $\frac{1}{4}$ Mesh Model

A more sophisticated standard SW 2D axisymmetric model consists of the indenter and material as before, but this time a Pressure Foot (PF) tool (nose piece) and spring simulating the action of the PF are added. The pressure foot is a cylindrical concentric to the indenter tool that applies a prescribed load to the area around the SW dimple during the indentation process.

The purpose of the PF tool is to provide restraint of the area immediately surrounding the indenter (dimple), while stabilizing the part being cold worked so that it remains normal to the indenting direction. The restraint provided around the area to be cold worked minimizes surface upset (albeit small without a PF). The stabilizing aspect of the pressure foot compensates for any axial mis-alignment of opposing indenters.

The PF concept involves a mechanism which can restrain the part near the area being SWCW with an appropriate constant load, while the indenter continues its penetration into the part, under increasing load, producing the requisite cold working (Figure 16). An alternative description of the PF would be a linear clutch.

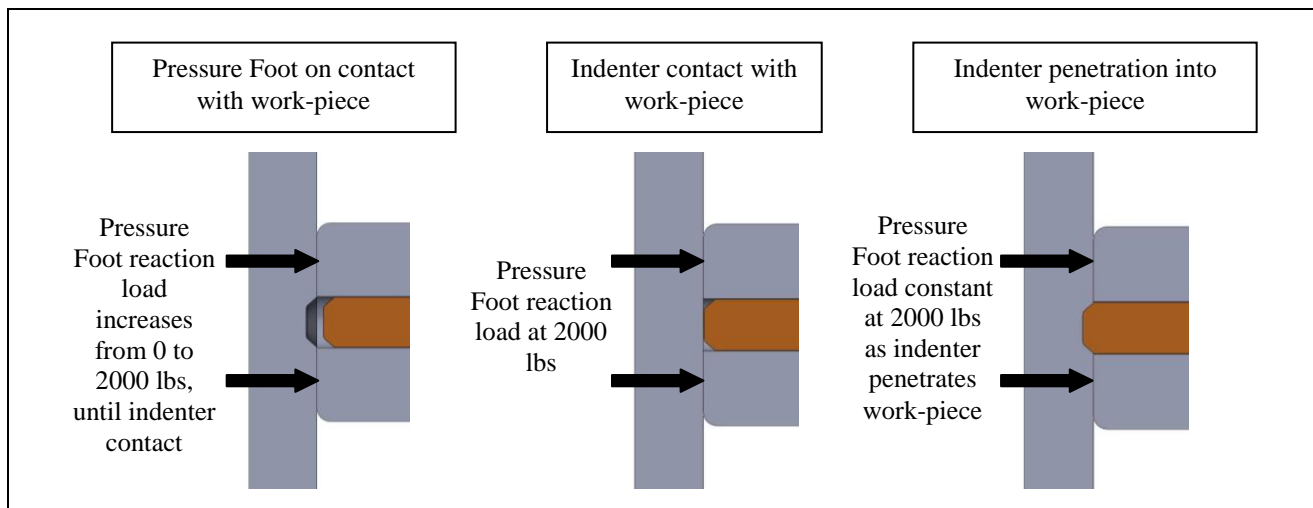


Figure 16. Pressure Foot Tool Schematic

Element model views of the PF tool are shown in Figures 17 and 18. For clarity, only half of the model is shown.

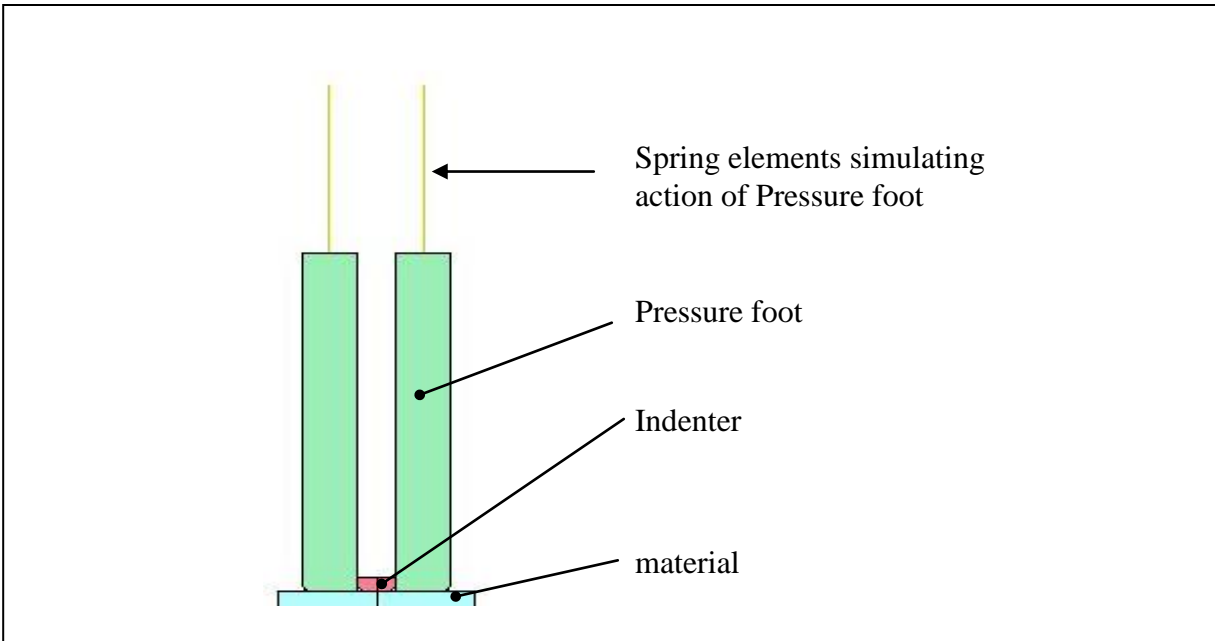


Figure 17. Element Model View – Pressure Foot Tool (1/2 View)

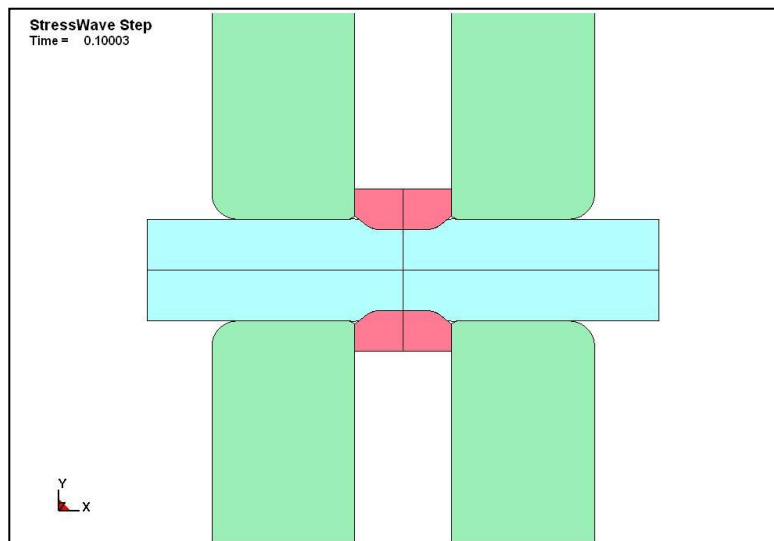


Figure 18. Element Model View – Pressure Foot Tool (Full View)

3.6 Material Models

The accuracy of any model depends on the accuracy and realism of the model and boundary conditions including sliding interfaces and frictional coefficients. Perhaps the biggest effect on the residual stresses computed by the program is the material behavior especially the post-yield behavior.

LS-Dyna requires that the yielding behavior be in units of true stress and true strain. Most data, especially those found in MIL-HDBK-5 (Ref.1), is in units of engineering stress and strain. Fortunately, there is a relatively straight forward calculation of true stress/strain from engineering stress/strain. In cases where the full stress-strain curve has been provided the data is converted from engineering to true units and input into LS-Dyna keyword file. Unfortunately, there is a surprising lack of full stress-strain curves in the public domain. Since SWCW involves significant plastic deformation of the metal it is important to obtain post-yield mechanical data. To overcome this lack of post-yield behavior data full stress-strain curves have been estimated using the Ramberg-Osgood equation. An example of the material model worksheet for 7085-T7651 is shown in Figure 19.

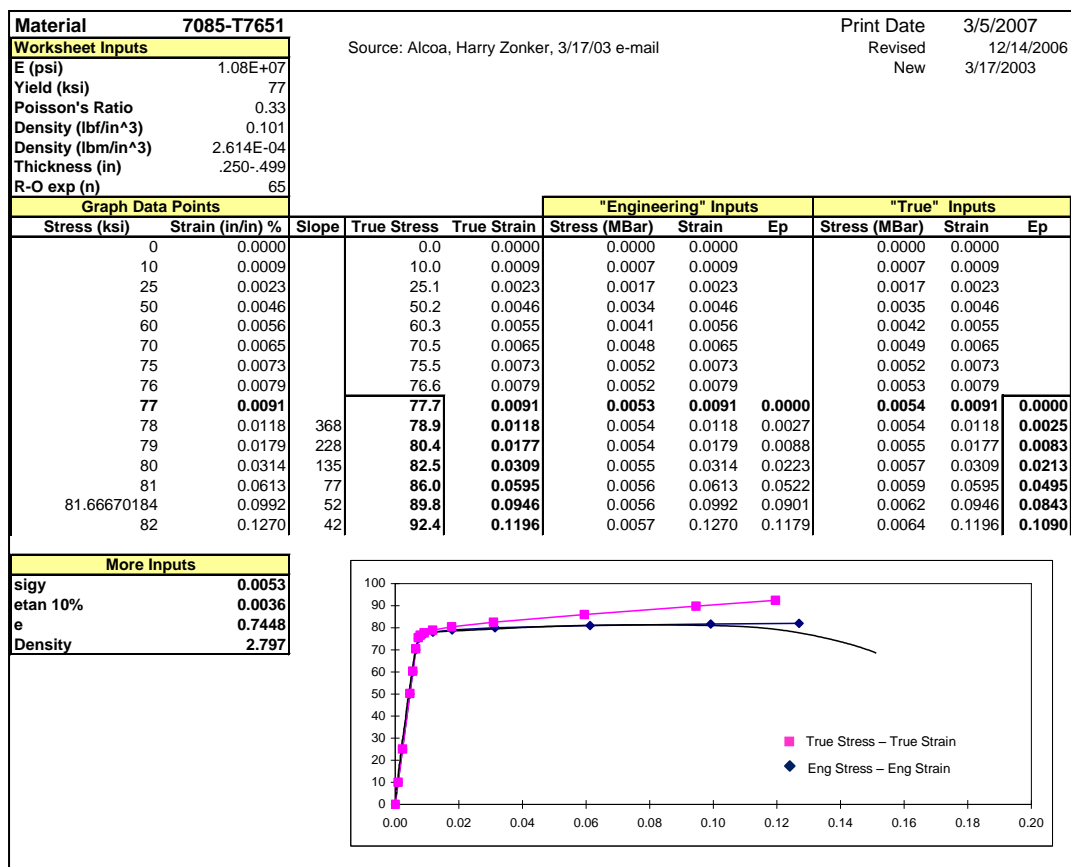


Figure 19. Material Model Worksheet

3.7 Hardening Model

Isotropic hardening has been used for all finite element analyses to date. It is known that isotropic assumption generally over-predicts both compressive and tangential stresses as illustrated in Figure 20. Because isotropic assumptions have been widely used in public domain reports and papers for cold work residual stresses, they are used as a means for comparison. LS-Dyna has the ability to control whether the solution runs using isotropic, kinematic or a combination of both by varying a beta parameter within the appropriate card within the LS-Dyna keyword file. The kinematic hardening only allows a bilinear curve, i.e., needs a tangent modulus.

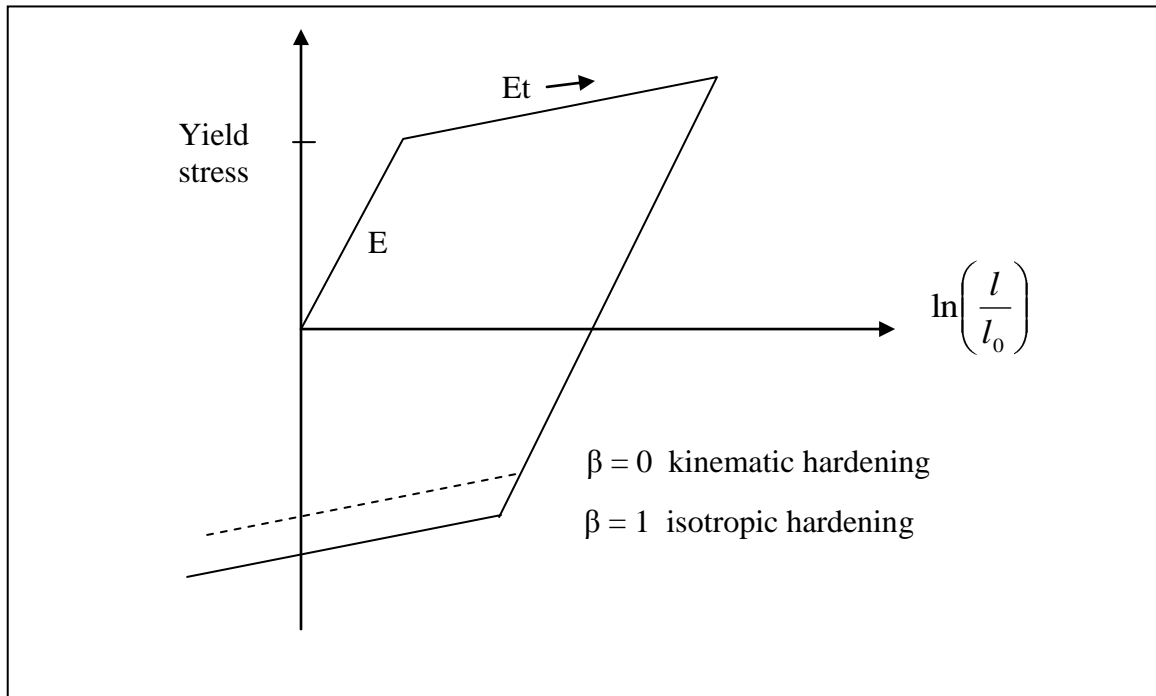


Figure 20. Isotropic Hardening vs. Kinematic Hardening

3.8 Results

The hoop stresses during maximum indenter engagement are shown in figure 21.

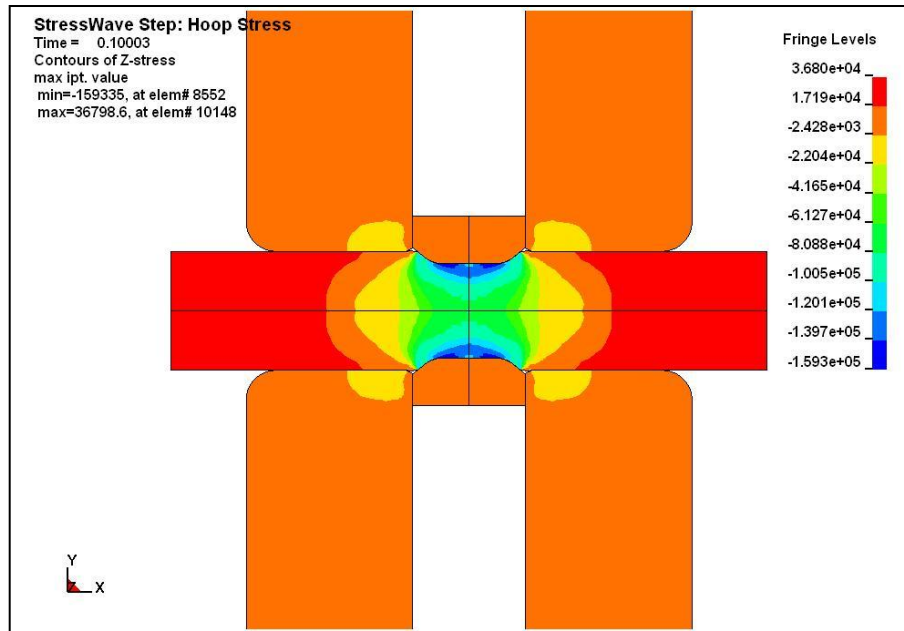


Figure 21. Hoop Stress, Maximum Indenter Engagement

The resulting residual hoop stress after indenting and hole cutting is shown in figure 22. The boundary between compressive hoop and tensile hoop stress is in the yellow region.

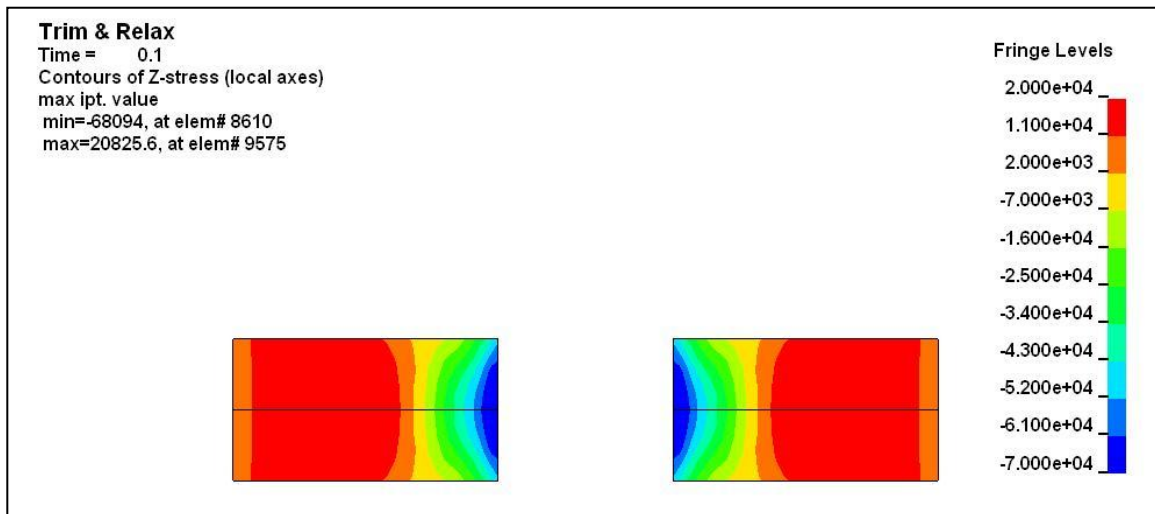


Figure 22. Resulting Hoop Stress, After Hole Cutting

A generic model of a rectangular pocket representing an F-35 bulkhead was made to review the stresses in 3 dimensions (Figs. 23-28). The model contains brick elements in of the components including the shape of the cup indenter shown in red. This model allowed for any shape and thickness of the pocket, height of the integral perimeter stiffeners as well as allowing positioning of the hole anywhere within the confines of the pocket.

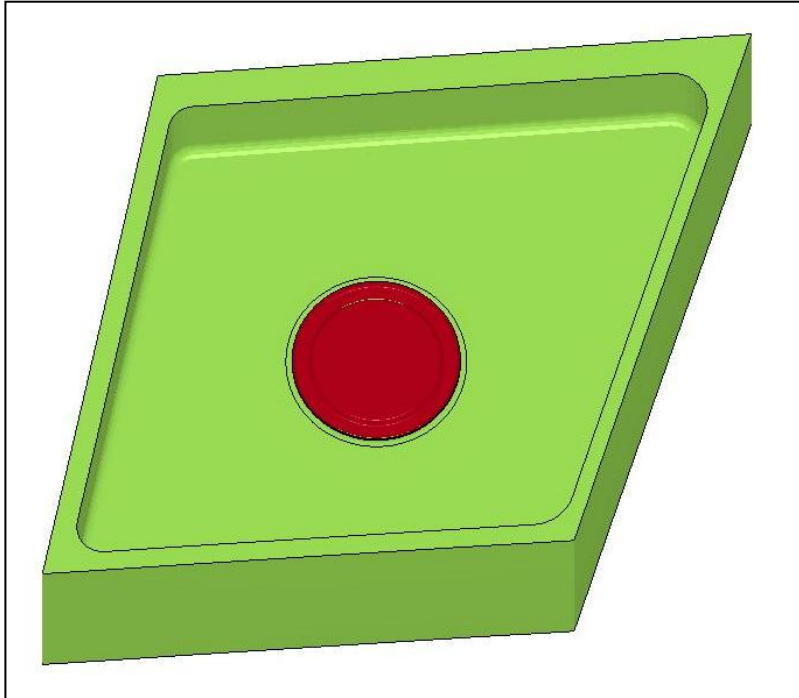


Figure 23. Generic Pocket FE Model

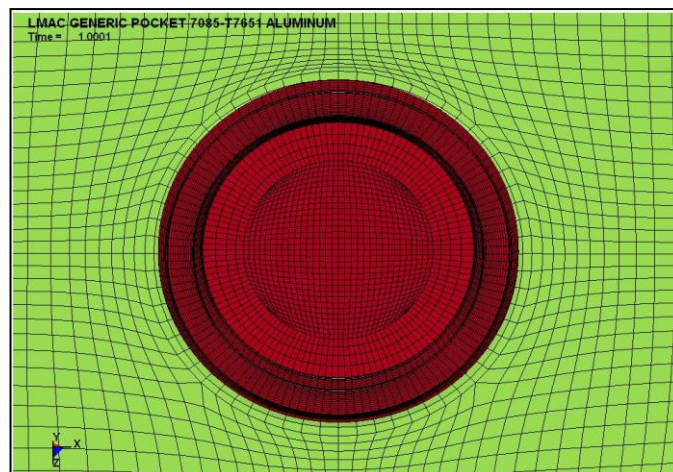


Figure 24. Close Up of Indenter (red) and the Mesh Details at the Hole

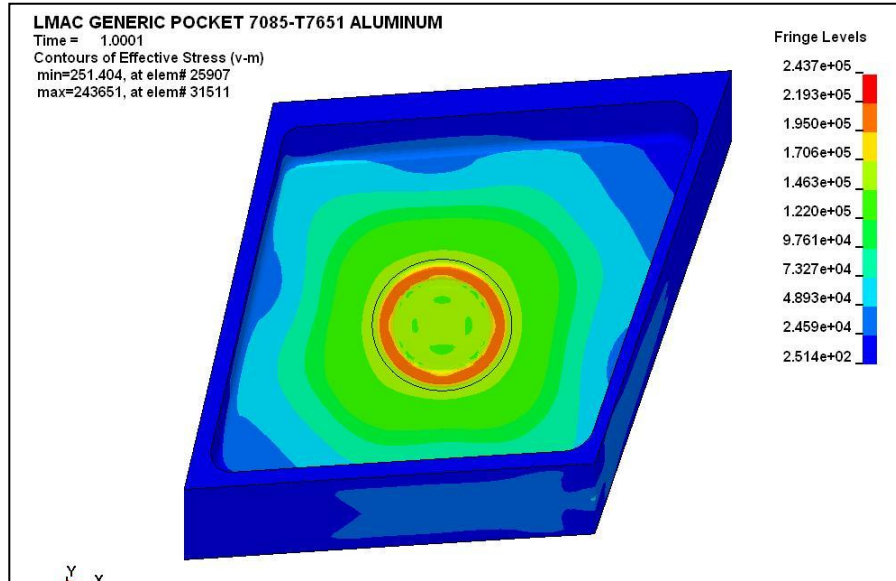


Figure 25. Von-Mises Stresses of the Pocket at Full Indenter Engagement

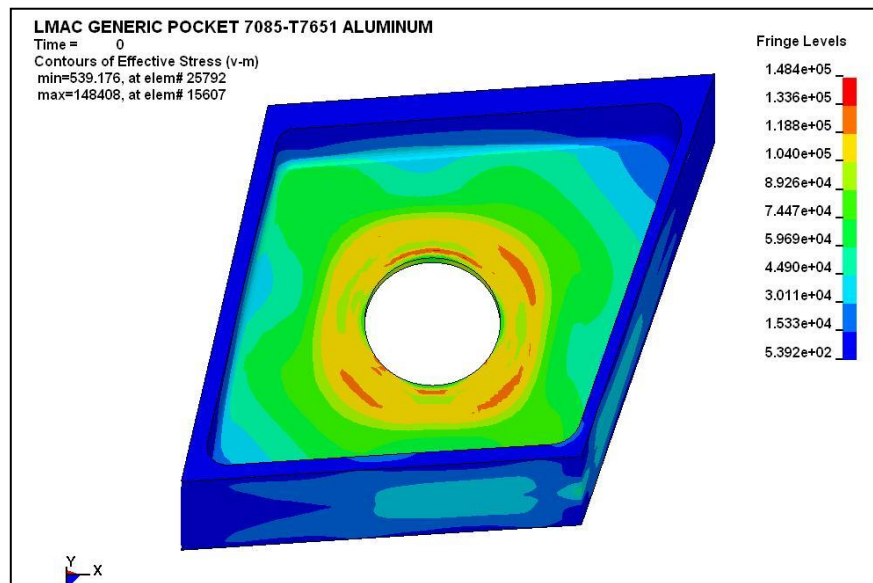


Figure 26. Von Mises Stresses after Hole Trimming and Relax

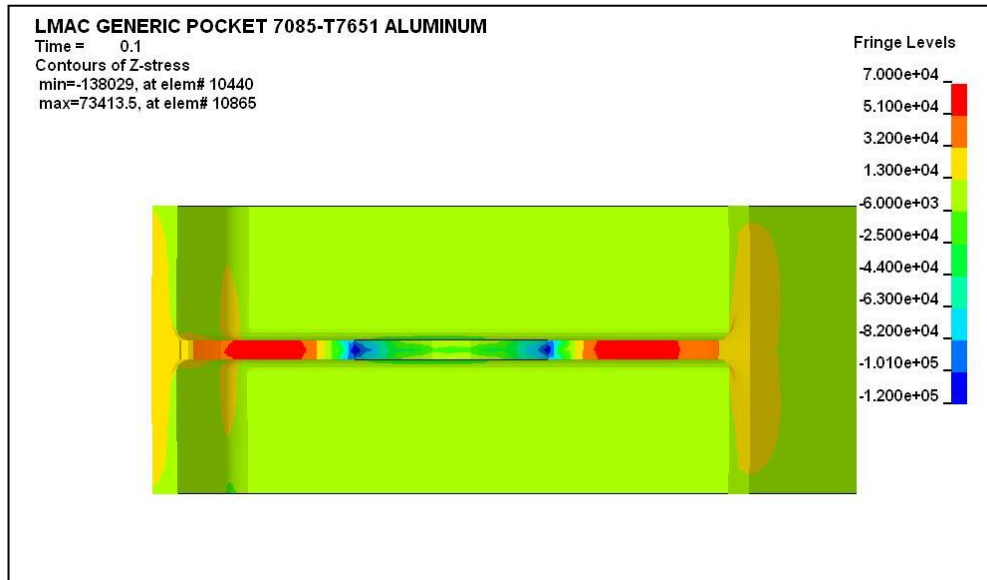


Figure 27. Hoop Stresses on Cut Section after Hole Trimming and Relax (Straight View)

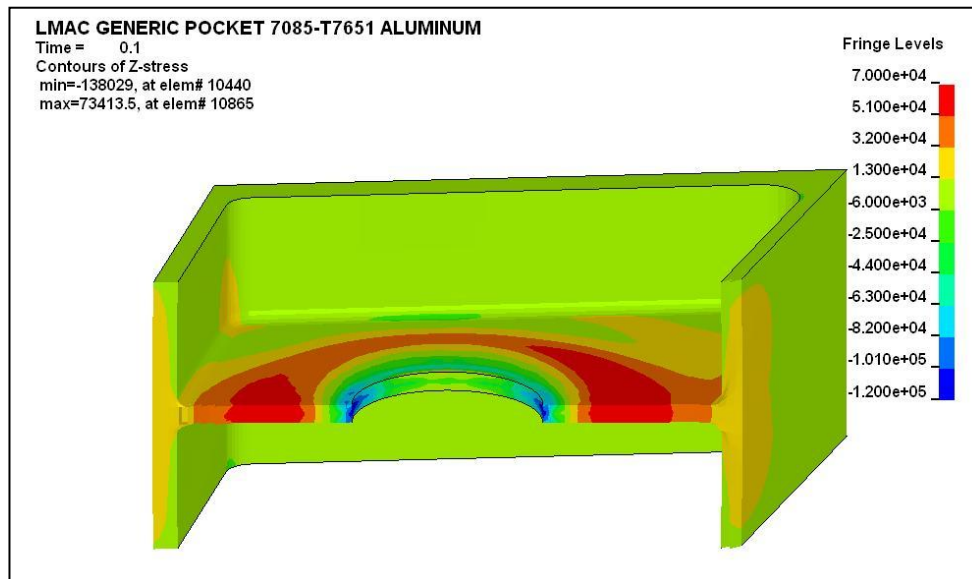
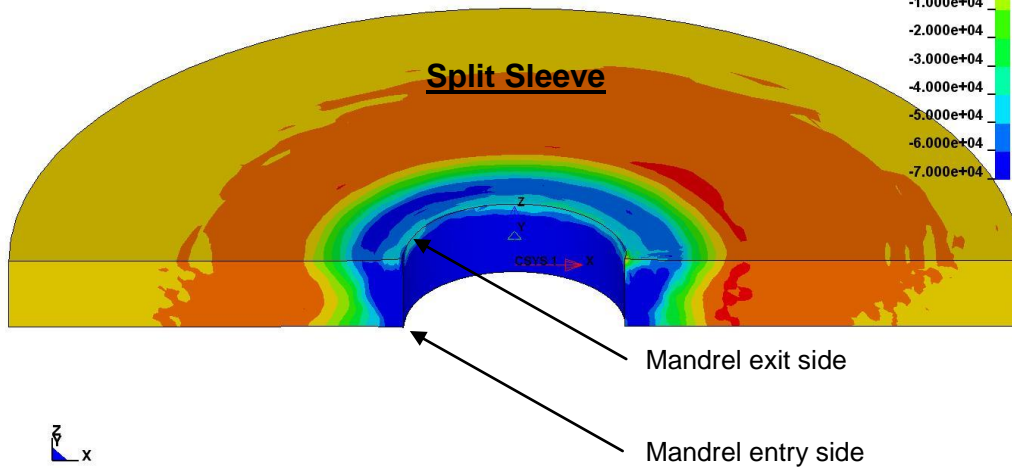


Figure 28. Hoop Stresses on Cut Section after Hole Trimming and Relax (Oblique View)

Using all of the information presented previously in Section 3, 3D comparison models were made of SWCW'd holes vs. split sleeve cold worked holes to validate process parameter and indenter design development work. A typical comparison is shown in Figure 29. The SWCW'd residual stress pattern exhibits extremely uniform through-the-thickness residual stresses as compared to the split sleeve residual stress pattern. The split sleeve residual stresses demonstrate the widely known “mandrel exit side vs. mandrel entry side” pattern of non-uniform stress distribution.

CX .438 HOLE, .105 THICK, 7085 Al
Time = 0.5
Contours of theta-stress (user local axes)
min=-110399, at elem# 869
max=31026.8, at elem# 3395

Fringe Levels
3.000e+04
2.000e+04
1.000e+04
0.000e+00
-1.000e+04
-2.000e+04
-3.000e+04
-4.000e+04
-5.000e+04
-6.000e+04
-7.000e+04



MILL & DRILL
Time = 0.4001
Contours of theta-stress (user local axes)
min=-67691.4, at elem# 16316
max=29426.4, at elem# 16730

Fringe Levels
3.000e+04
2.000e+04
1.000e+04
0.000e+00
-1.000e+04
-2.000e+04
-3.000e+04
-4.000e+04
-5.000e+04
-6.000e+04
-7.000e+04

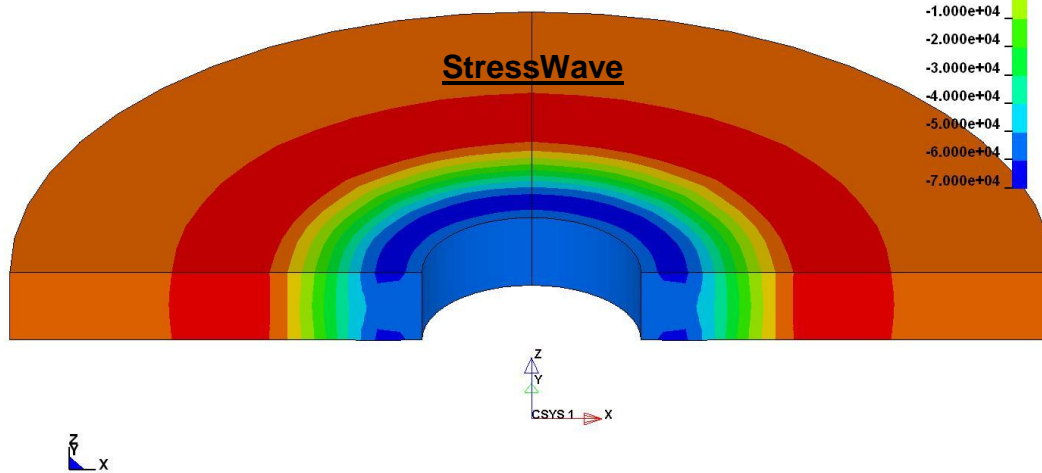


Figure 29. Comparison of Residual Stresses, StressWave and Split Sleeve (1.125 Inch Diameter Hole)

4.0 Test Program

4.1 Test Program Introduction

The test program consisted of room temperature constant amplitude fatigue testing on open hole zero load transfer coupons made from 7085 and 7050 aluminum plate, in the longitudinal-transverse (LT) and longitudinal-short transverse (LS) grain directions, designed to simulate bulkhead geometries, or replicate LM cold working qualification tests as described in Ref. 14. Note that a specimen with a LS grain orientation corresponds to the condition of having the hole cold worked in the short transverse (ST) grain direction.

Constant amplitude testing was performed with open hole, zero load transfer specimens under constant amplitude load conditions (R ratio = .05), as shown in Table 1, using 7050 and 7085 plate. Three applicable geometries were tested. The first was 0.250 inch holes in 0.250 inch thick, a typical specimen geometry simulating many applications of cold working. The second was 0.4375 inch open holes, using similar test coupon thicknesses and load conditions as shown in Ref. 2. The third was 1.125 inch diameter open holes using a thickness simulating a penetration hole in a F-35 bulkhead.

Table 1. Constant Amplitude Test Conditions (R = 0.05)

Material	Grain Direct	Nominal hole size, in	Nominal thickness, in	Maximum stress, PSI
7085-T7651	LT	0.250	0.25	30,000
				35,000
		0.438	0.15	30,000
				35,000
		1.125	0.22	30,000
				36,000
	LS	0.250	0.25	30,000
				35,000
7050-T7451	LT	0.250	0.25	30,000
				35,000
		0.438	0.15	30,000
				35,000
		1.125	0.22	30,000
				36,000
	LS	0.250	0.25	30,000
				35,000

Each series of tests was comprised of at least four, but normally six, coupons. There were nearly 300 total coupons in the constant amplitude fatigue tests.

4.2 Specimen Preparation

The Alcoa Technical Center, Pittsburgh, PA, supplied pieces of 7085-T7651 and 7050-T7451 aluminum plate material for use in the test program. These pieces were rough sawn into specimen blanks that were approximately 3.0" (or 3.5") x 12.0" x 0.5" inches. These blanks were then double disk ground into 64R_a finish provisional blanks from which final specimen geometries could be fabricated. Some blanks were then profiled to a reduced section width for the 0.25 inch hole diameter tests. Blanks were cut from the plate for testing in the longitudinal-transverse grain direction (LT), and in the longitudinal short-transverse grain orientation (LS) as illustrated in Figure 30. The short transverse grain direction (S) aligns the tensile and compressive residual stress fields in the worst possible orientation. The short-transverse grain direction is considered the usual specimen grain orientation. Every specimen blank was uniquely identified at this time by steel stamping or vibro-etching. Specimen blanks are shown in Figure 31. Final specimen dimensions are shown in Figure 32.

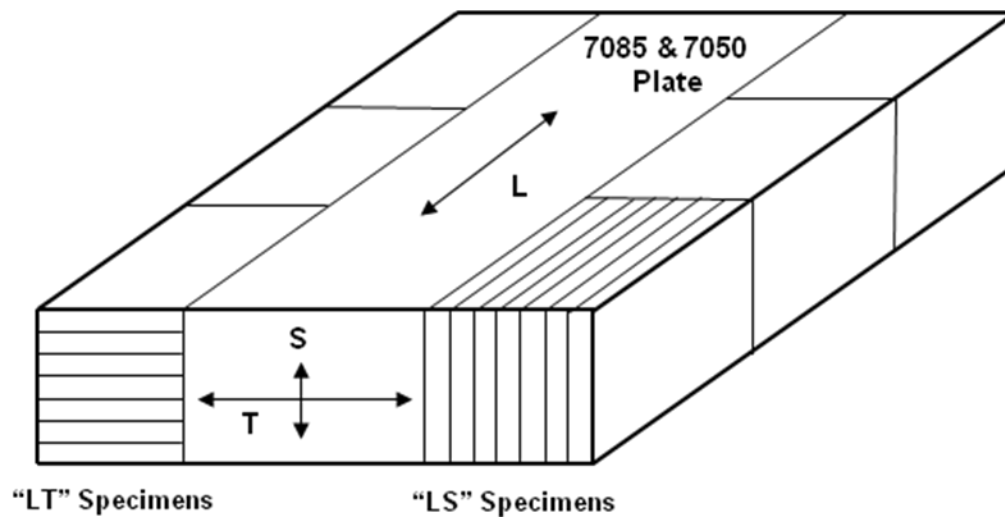


Figure 30. Cut diagram for “LT” & “LS” specimen orientations from 7085 & 7050 plate.

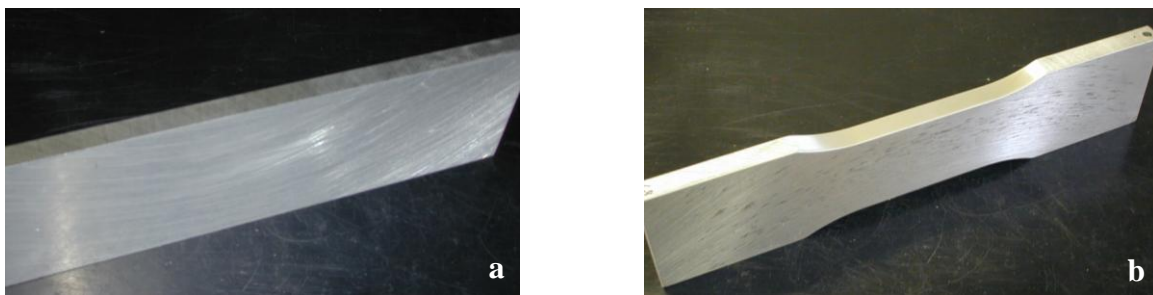
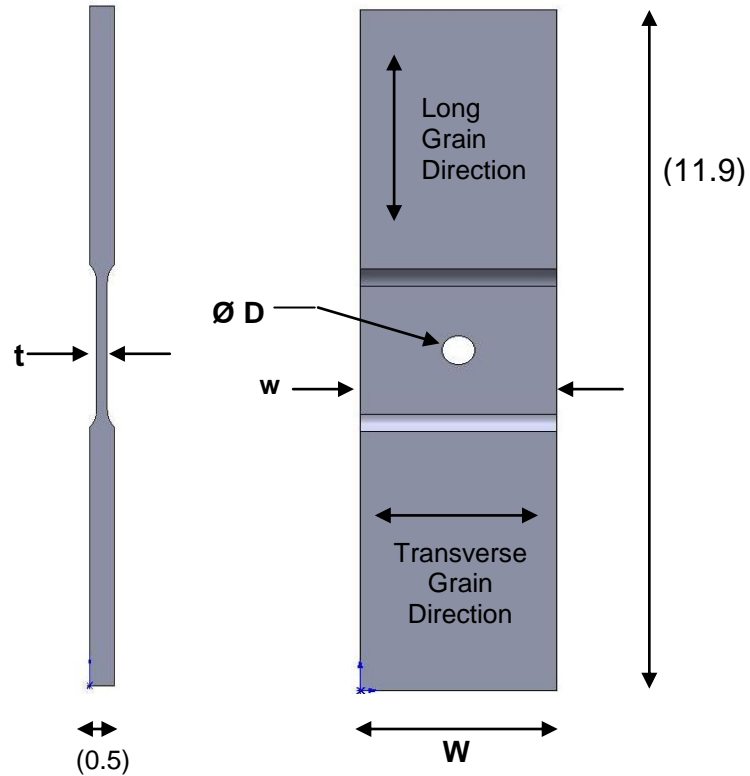


Figure 31. Specimen blanks as cut from plate (a) and prior to cold working (b).



All dimensions are nominal, in inches

Alloy	Specimen final hole diameter $\varnothing D$	Grain Orientation	Specimen blank width W	Test section thickness t	Test section width w
7085-T7651 Plate	0.250	L	3.0	0.250	2.0
	0.4375			0.150	3.0
	1.125			0.224	3.0
	0.250	S	2.6	0.250	2.0
7050-T7451 Plate	0.250	L	3.5	0.250	2.0
	0.4375			0.150	3.5
	1.125			0.224	3.5
	0.250	S		0.250	2.0

L = Longitudinal
T = Transverse
S = Short Transverse

Figure 32. Fatigue Specimen Dimensions

Baseline (non-treated) specimens were prepared by milling the test section in the specimen blank to the appropriate thickness and then drilling and reaming the appropriate size hole.

Split sleeve specimens were prepared by drilling the appropriate starting hole per Ref. 14 (0.250 inch and 0.4375 inch holes) or Ref. 15 (1.125 inch holes). The 0.250 inch and 0.4375 inch diameter hole specimens were split sleeve cold worked using the correct Standard Tool Diameter Number (STDN) mandrel and split sleeves, per the instructions in Ref. 14. The nominal applied expansion for these smaller diameter holes ranged from 3.65% to 3.75%. Holes in these specimens were then reamed to the final hole diameter (Figure 26) per Ref. 14. The 1.125 inch diameter split sleeve specimens were sent to Progressive Industries, Arlington, TX, where the split sleeve cold working was done using production tooling for the F-35 bulkhead per Ref. 15. The applied expansion for these holes is proprietary to Lockheed Martin. These holes were not reamed after cold working, per Lockheed Martin instructions (the cold worked hole diameter is the correct size). Split sleeve cold working was performed with the split in the sleeve aligned at 90° to the direction of applied loading, which is customary for this specimen design.

SWCW specimens were prepared by indenting the target areas with the appropriate SWCW indenter, in the initial test section blank thickness (nominally 0.5 inches). A typical set-up for SWCW indenting (dimpling) in the laboratory is shown in Figure 33. The “pressure foot” concept is used, which helps to restrain the material around the area of the dimple. Typical dimples for each size specimen are shown in Figure 34. The indenter for the 1.125 inch hole is a different design than the indenters for the 0.250 and 0.4375 inch holes, due to the size.



Figure 33. Typical SWCW Indenting Setup



Figure 34. Specimen Dimples (1.125 in, 0.4375 in, and 0.250 in)

After dimpling, the specimens were then milled to the required final test section thickness, and the appropriate holes drilled and reamed. All the holes in all specimens were hand de-burred. A typical sequence of SWCW specimen assembly, from blank to final hole, is shown in Figure 35.

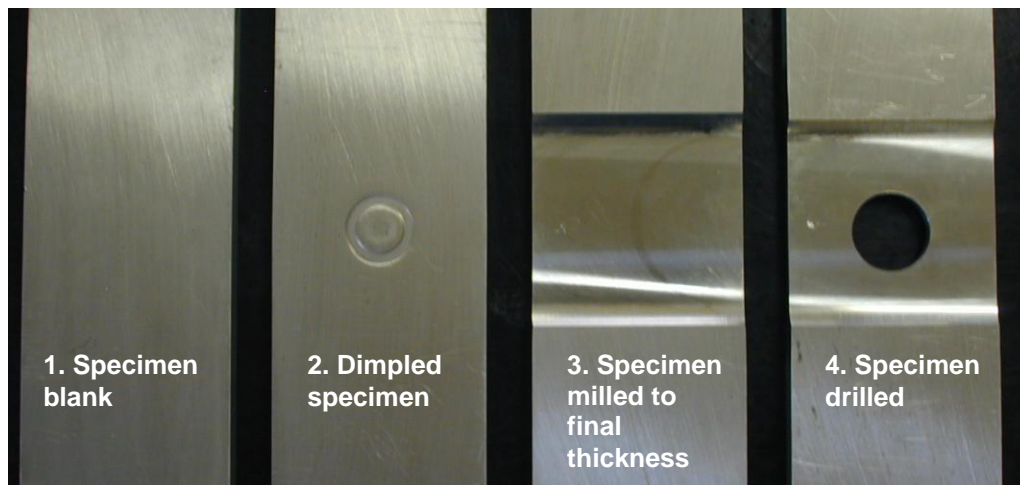


Figure 35. SWCW Specimen Assembly (1.125 inch hole shown)

4.3 Fatigue Testing

4.3.1 Test Protocol

Testing was performed at room temperature and under constant amplitude loading conditions, at a stress ratio (R) = .05 at a frequency of 20 Hz. Specimens were cycled to two-piece failure, or failure to hold load within 2% of amplitude range. All testing was performed in a closed-loop, electro-hydraulic fatigue test machine, calibrated periodically using standards traceable to the National Institute of Standards and Technology (NIST). A typical test setup is shown in Figure 36.



Figure 36. Typical Constant Amplitude Test Setup

4.3.2 Test Results

Results for constant amplitude testing are shown in Figures 37-44, and in Table 2. Any specimen reaching 1,000,000 cycles was terminated as a “No failure”. Typically, as seen in other tests of long running specimens, there were a number of failures away from the hole, in the grip area or other transition areas. Specimen finishing methods (edge finishing, etc.) were employed to reduce these failures to a minimum. The trends are unambiguous and clearly demonstrate that upstream SWCW in near net shape condition (Upstream Cold Working) provided significantly longer lives than split sleeve cold working, for the conditions tested.

Table 1 provides test results as fatigue life improvement factors (LIF). The LIF is the ratio of the fatigue life of a cold worked specimen to a baseline, non-cold worked specimen. Split sleeve specimens demonstrated between 1.26:1 and 4.1:1 life improvement (cold worked life:non-cold worked life) as compared to baseline non-treated specimens, for the test stress levels, hole diameters, and grain directions tested. These results are fairly consistent with the exhaustive testing performed over 40 years with split sleeve cold working, demonstrating, typically, minimum 3:1 life improvement. The SWCW specimens demonstrated between 2.2:1 and over 40:1 life improvement as compared to the baseline, non-treated specimens, for the test stress levels, hole diameters, and grain directions tested. The SWCW specimens LIF's, as compared to split sleeve LIF's, demonstrated a minimum improvement of 80% to a maximum improvement of over 1300%.

**Table 2. Minimum Constant Amplitude Fatigue Life Improvement Factors (LIF),
StressWave Cold Working (SWCW) vs. Split Sleeve (SS)**

Open Holes

Material	Grain	Nominal hole size, in	Nominal thickness, in	Maximum stress¹, PSI	Minimum LIF², SS	Minimum LIF, SW	SW improvement vs SS, % (Upstream SW)
7085-T7651 Plate	LT	0.250	0.25	30,000	4.53	20.42	351%
				35,000	2.64	18.29	593%
		0.438	0.15	30,000	2.95	47+ (NF ³)	586%
				35,000	4.12	43.75	962%
		1.125	0.22	30,000	3.77	15.87	321%
				36,000	1.69	2.76	63%
	LS	0.250	0.25	30,000	3.00	20.25+ (NF)	575%
				35,000	2.26	31.28	1284%
7050-T7451 Plate	LT	0.250	0.25	30,000	3.27	44.56	1263%
				35,000	3.54	10.02	183%
		0.438	0.15	30,000	2.87	16.53	476%
				35,000	3.29	8.10	146%
		1.125	0.22	30,000	2.76	11.73	325%
				36,000	1.26	2.28	81%
	LS	0.250	0.25	30,000	3.06	45.26+(NF)	1379%
				35,000	2.34	9.65	312%

¹ R = .05

² LIF = Minimum Split Sleeve or StressWave fatigue life divided by baseline (non-treated) life

³ NF = No failures

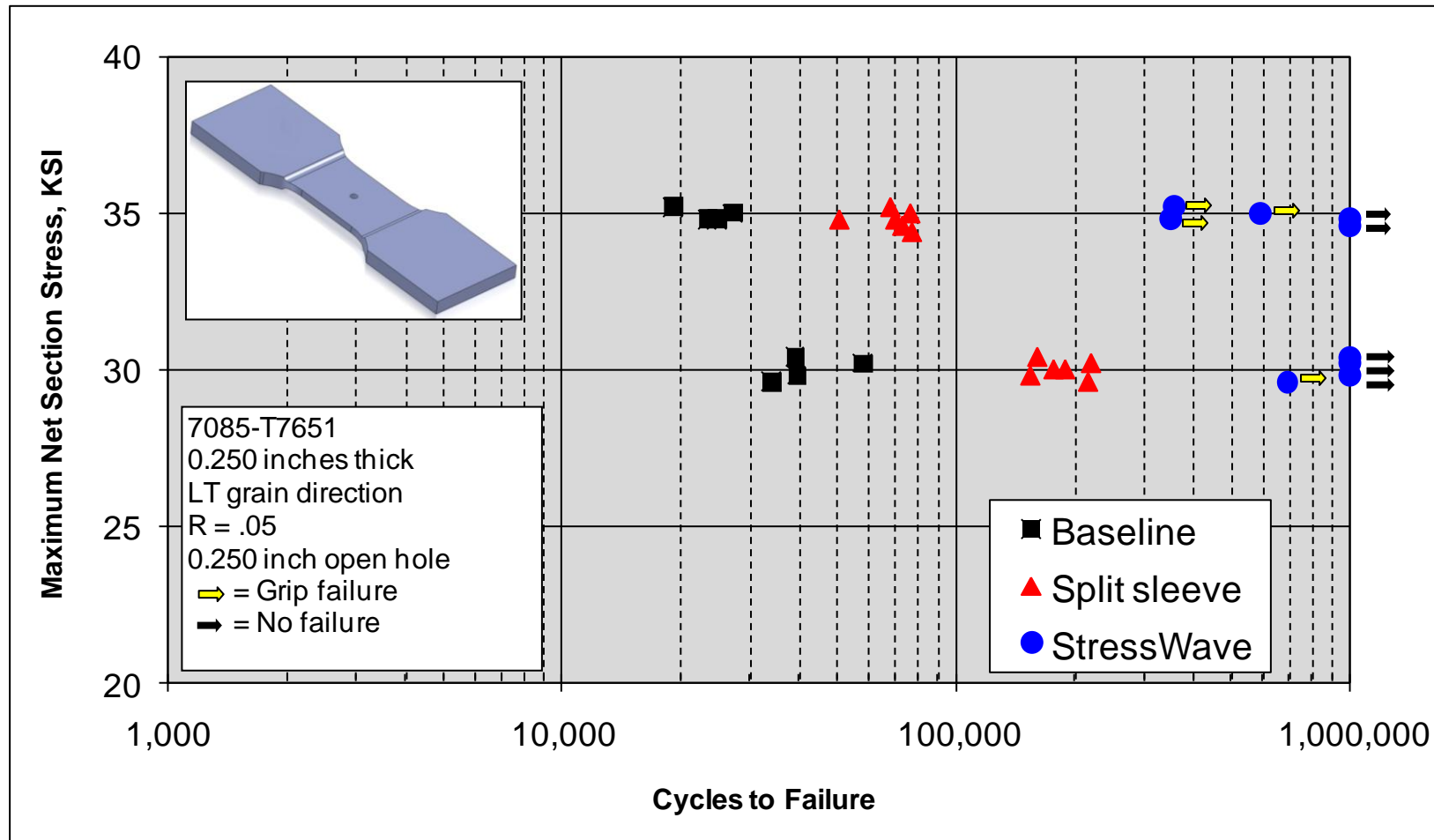


Figure 37. Constant Amplitude Fatigue Test Results – 7085-T7651 – 0.250 inch –LT Grain Orientation

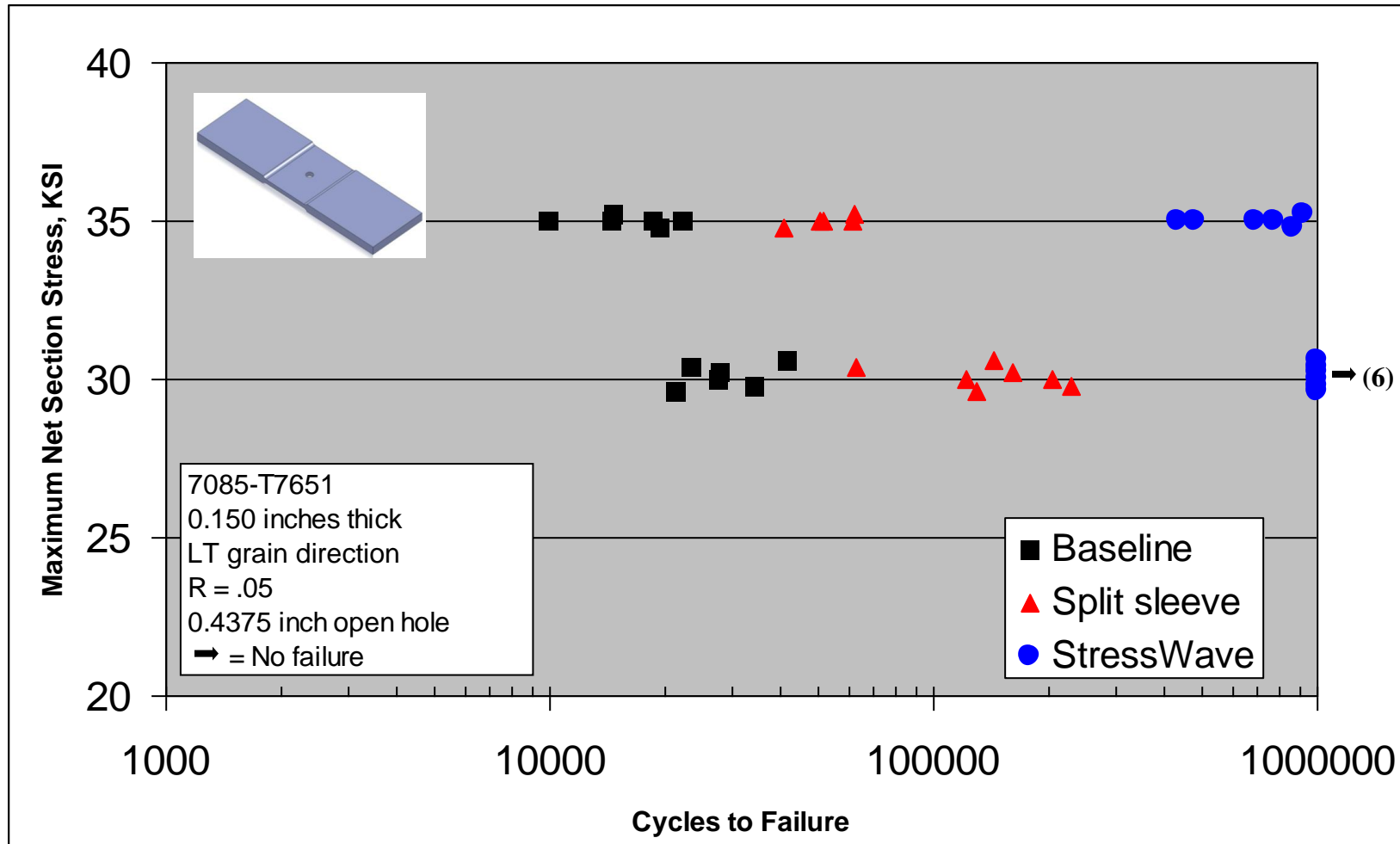


Figure 38. Constant Amplitude Fatigue Test Results – 7085-T7651 – 0.4375 inch – LT Grain Orientation

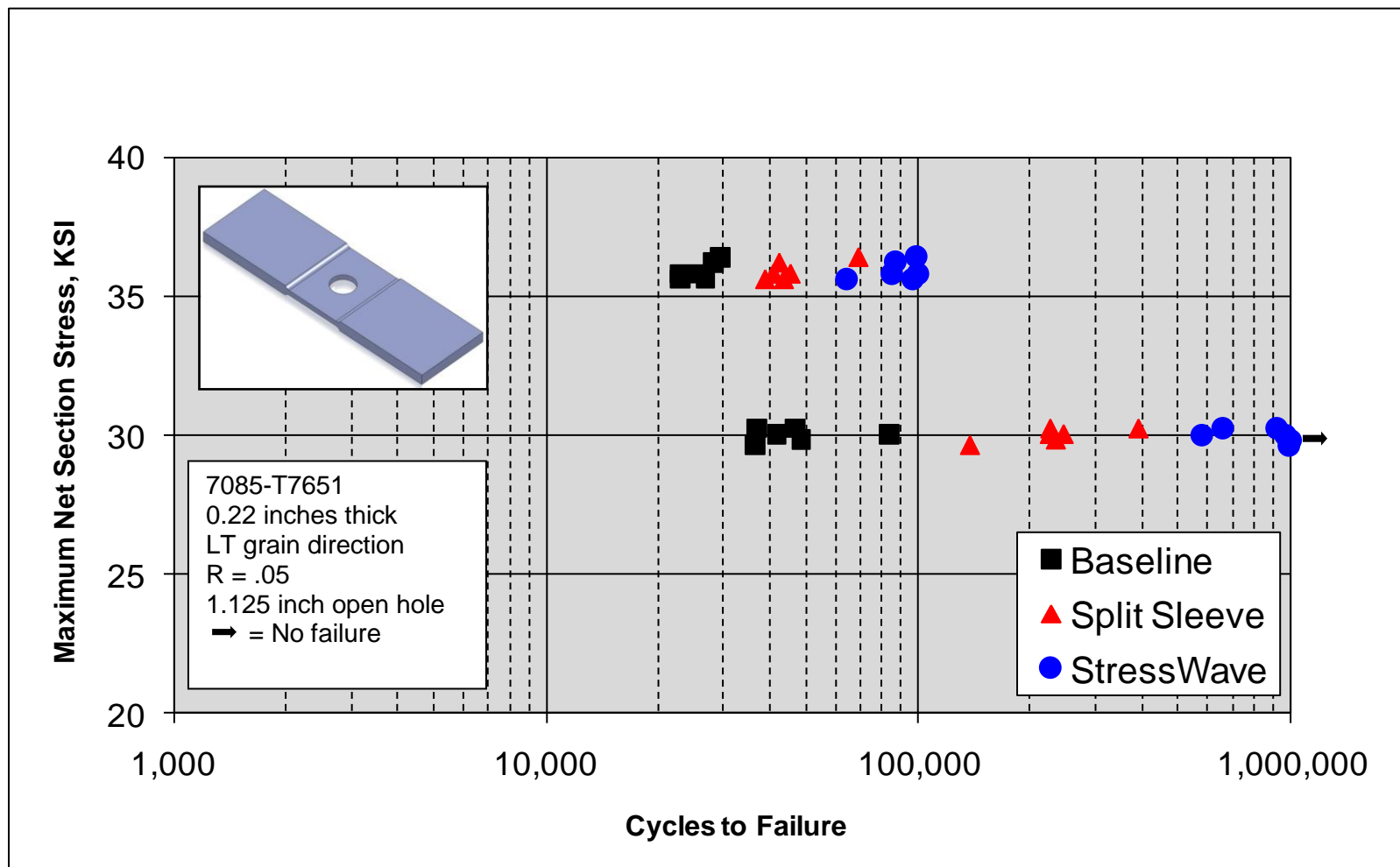


Figure 39. Constant Amplitude Fatigue Test Results – 7085-T7651 – 1.125 inch –LT Grain Orientation

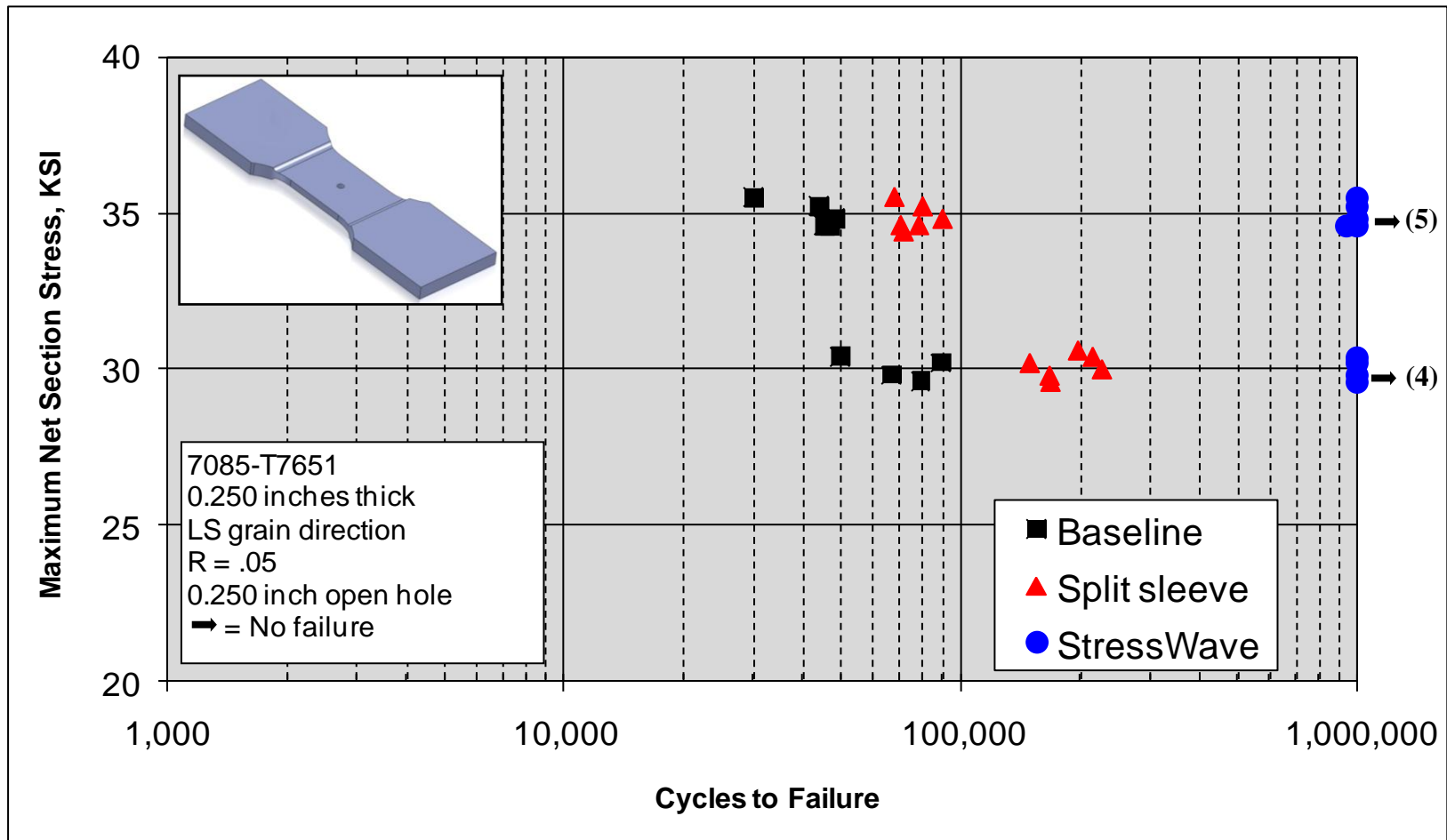


Figure 40. Constant Amplitude Fatigue Test Results – 7085-T7651 – 0.250 inch –LS Grain Orientation

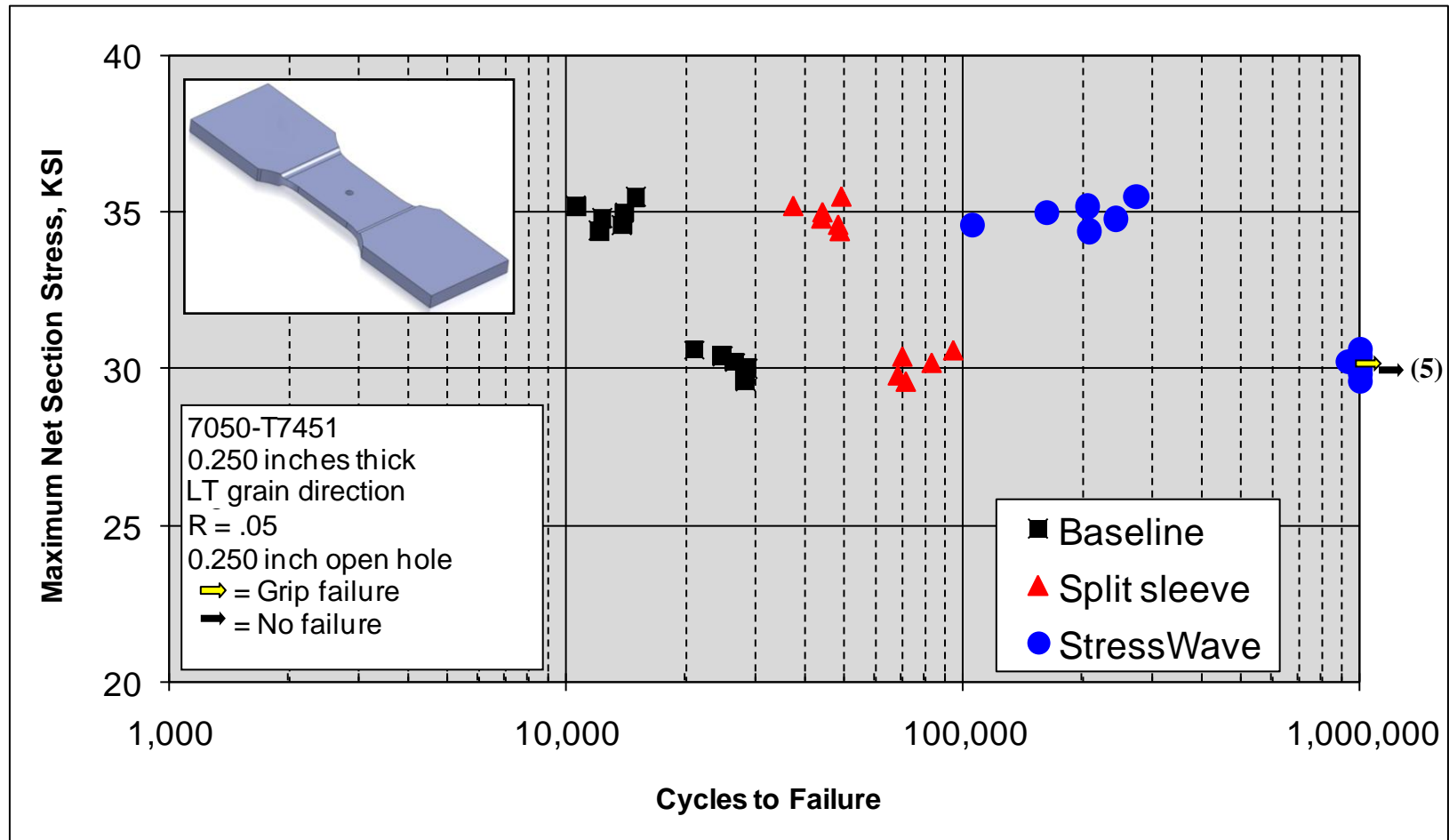


Figure 41. Constant Amplitude Fatigue Test Results – 7050-T7451 – 0.250 inch – LT Grain Orientation

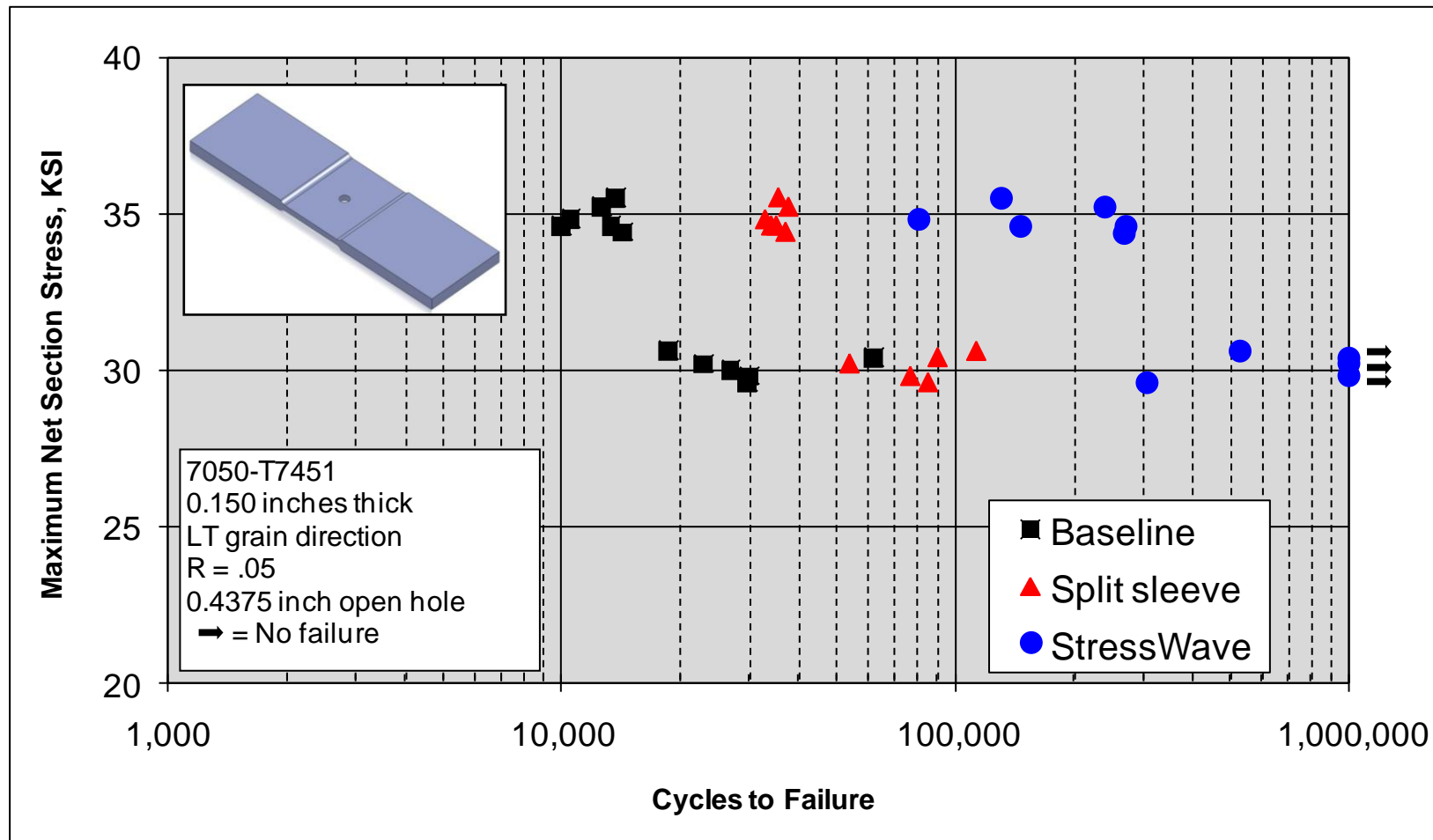


Figure 42. Constant Amplitude Fatigue Test Results – 7050-T7451 – 0.4375 inch –LT Grain Orientation

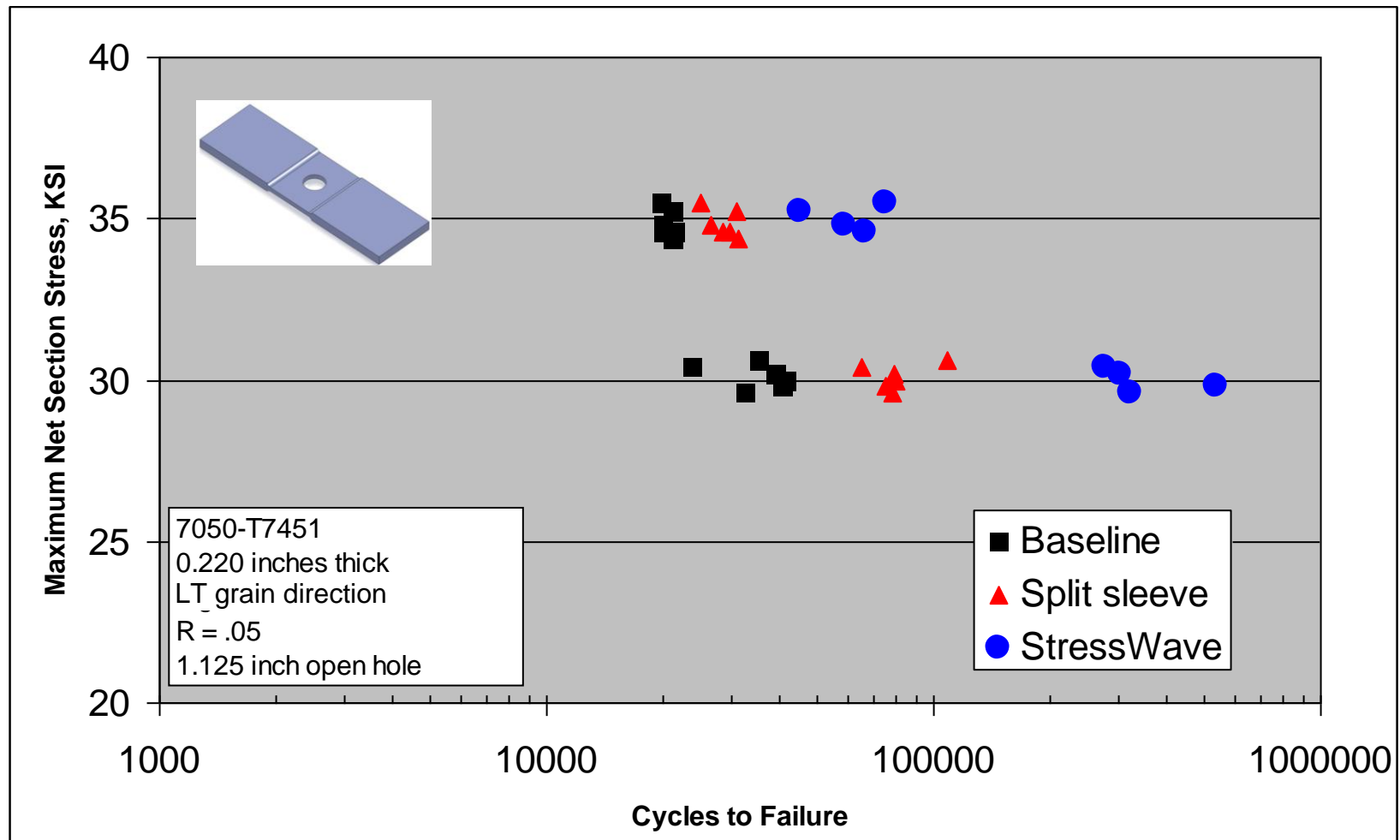


Figure 43. Constant Amplitude Fatigue Test Results – 7050-T7451 – 1.125 inch –LT Grain Orientation

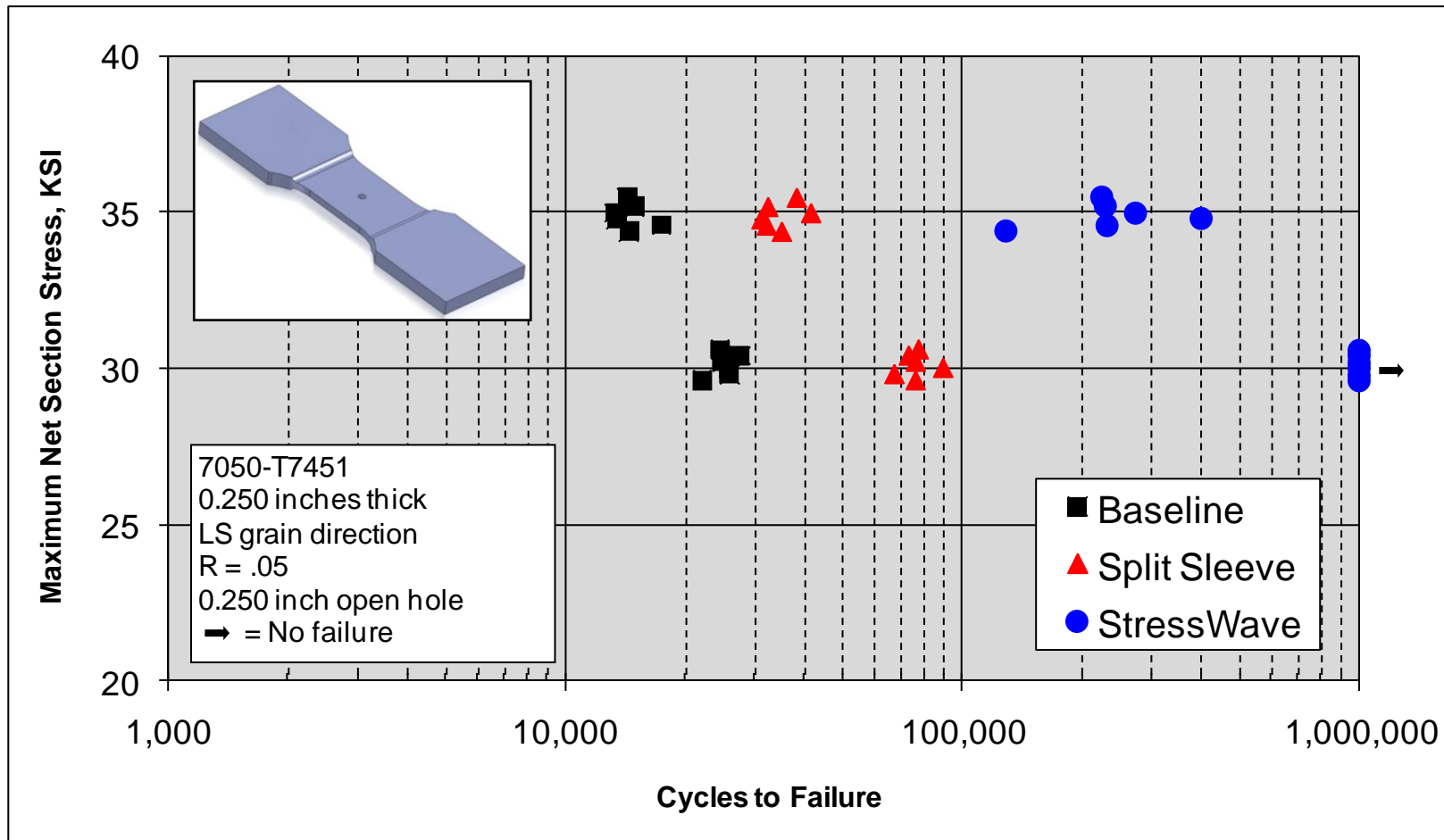


Figure 44. Constant Amplitude Fatigue Test Results - 7050-T7451 – 0.250 inch –LS Grain Orientation

5. Tooling Development

5.1 Tooling Development Introduction

Discussions with many OEM companies have revealed that the commercialization of SWCW has been restricted due to the lack of tooling development. Tooling development, in a number of different forms, will be required before widespread usage can begin. Hence, the tooling development phase of the program consisted of three main tasks, each designed to provide a basis for production of implementation tooling that would be adaptable for specific applications. Operating proof-of-concept tools were developed for two of the concepts, the Portable Manual Tool, and the On-Device Tool. Although proof-of-concept development of a fully automated stand-alone SWC tool was beyond the scope of the current effort, preliminary system design and testing of one of the higher risk parts of a potential system (Z-axis compliance) was accomplished.

SWCW requires three hardware elements; indenter(s), a means of applying force, and a positioning system. Any concept for SWCW, including the tooling developed and/or prototyped in this effort, must include these elements. Additionally, tooling variations may be required for particular applications or implementation method. Of these variations, the PF concept which was previously discussed in Section 3.5 (Figure 16) has been shown to be important. The PF provides restraint of the area immediately surrounding the indenter (dimple), while stabilizing the part being cold worked so that it remains normal to the indenting direction. The restraint provided around the area to be cold worked minimizes surface upset (albeit small without a PF). The stabilizing aspect of the pressure foot compensates for any axial mis-alignment of opposing indenters.

An unusual complication of designing a PF is the requirement that the device requires a spring mechanism that is high load, high displacement, and contained within a small volume. These are often contradictory requirements for spring systems. Various alternative mechanisms were investigated for providing these requirements, including mechanical springs, mechanical cams, hydraulic systems, electrical systems, and elastomeric compounds. After investigation, it was determined that a hydraulic system offers the best combination of accuracy and repeatability, albeit with some complication due to the use of hydraulic fluids.

5.2 On-Device (End Effector) Tool

The objective of this task was to enhance an early design end effector which could be used for integration into a robotic assembly device or press system. The end effector incorporates the indenter into a tool that can be mounted on a device which provides the necessary applied force. A PF is highly desirable, and early design efforts produced an end effector which used mechanical disc (Belleville) springs for the PF (linear clutch mechanism) described previously (Figure 45). Disc springs, although capable of providing the high load, high displacement characteristics required, are unreliable and inconsistent. This design was considered suitable for lab work only, requiring many adjustments to the mechanism depending on application requirements.

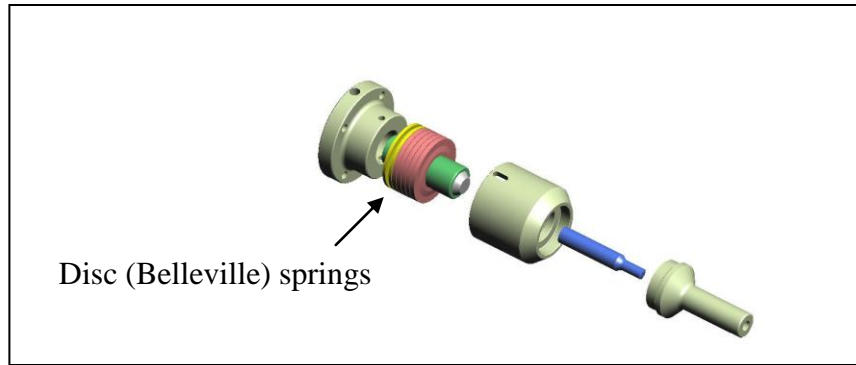


Figure 45. Early Design End Effector

After consideration of other mechanical systems, it was decided to base a new PF design on a hydraulic system, due to the ability of hydraulics to consistently and repeatedly produce high loads in a small volume. This design uses a dual chamber system similar to a shock absorber, consisting of a high and low pressure chamber, piston, and front and rear sealing end caps. The rear surface of the front end cap and the front surface of the piston form the high pressure chamber. Indenting force is applied to the end effector through the PF nosepiece, and as the nosepiece begins to make contact with the work-piece, pressure builds in the chamber until reaching a pre-set level (e.g., 500 psig). A relief valve cracks and vents the hydraulic fluid to the low pressure chamber formed by the rear of the piston assembly and the rear sealing end cap. The relief valve, which continues to crack and close between a high and low set point, allows the system to maintain a nearly constant load (a load of 2,000 pounds was used for baseline prototype development) on the PF nosepiece, as the indenting load increases. After indenting is complete, and load is removed from the end effector, a low pressure check valve allows the fluid to return to the high pressure chamber for the next cycle. Significant components of the end effector are shown in Figure 46 and 47, pictures of the proof-of-concept tools. A second generation prototype is planned, which will incorporate better sealing concepts and an easier fill and bleed mechanism.



Figure 46. Proof of Concept Hydraulic Pressure Foot End Effector

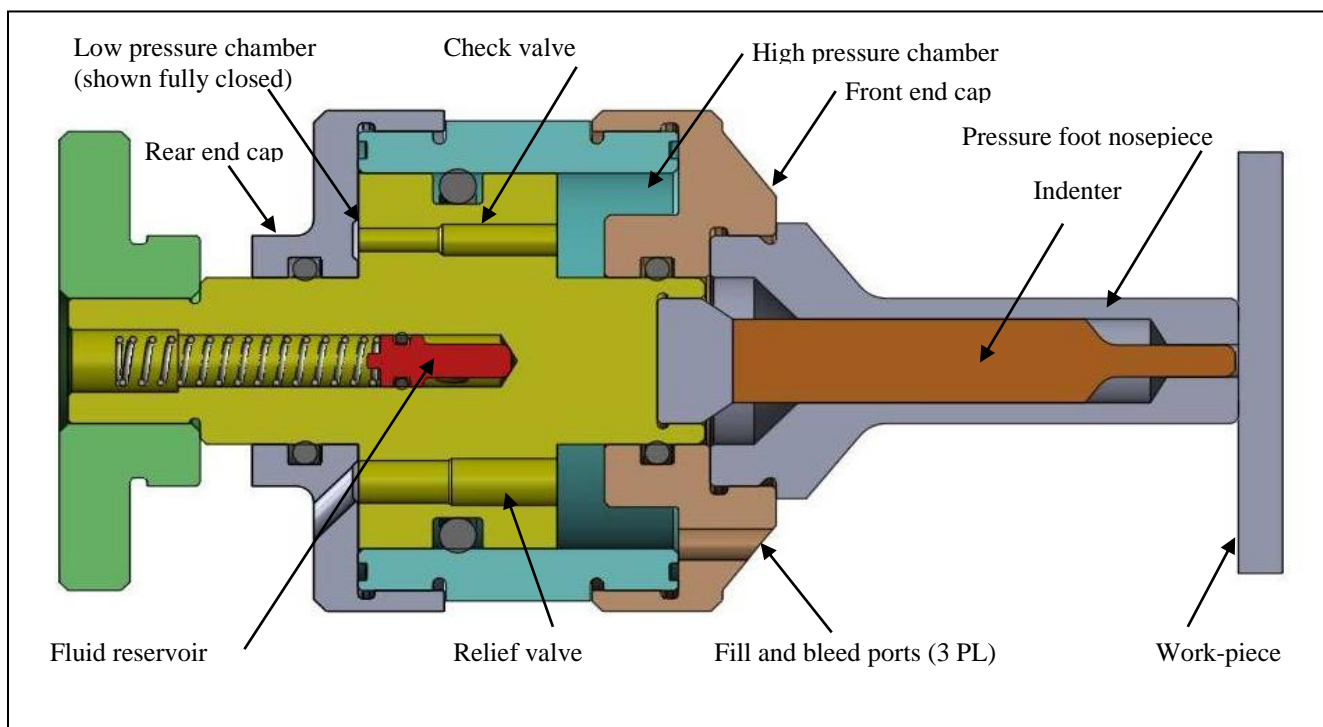


Figure 47. Schematic of Hydraulic Pressure Foot End Effector

5.3 Portable (On-Aircraft) Manual Tool

This type of portable tool, the equivalent of “puller units” for split sleeve or split manual cold working, would be used for on-aircraft SWCW. After review of concepts, a simple hydraulically powered C-yoke unit was designed and prototyped (Figure 48).



Figure 48. Portable Manual SWCW Tool

Although hydraulic power requires a hydraulic power supply (HPS), HPS units are readily available and are, in fact, in widespread usage for existing mandrel cold working methods. The SWCW C-yoke unit was designed to be able to use existing HPS units, which typically employ an air-logic control system to power the HPS on and off.

The proof-of-concept unit was designed, machined, and assembled. The capacity of the POC unit is 6,000 pounds, but the basic design is scalable up to approximately 20,000 pound capacity. Beyond 20,000 pounds, a unit of this type would be too heavy to operate manually, although larger capacity units could be accommodated with a counterbalance system.

5.4 Stand-Alone (Piece Part) Tool

The objective of this task was to begin design efforts for an automated SWCW tool for use in upstream cold working of structural parts, and to the extent possible, reduce the risk of full-scale development. Design efforts were based on a theoretical application used throughout this program for SWCW process parameter development; SWCW of F-35 wing carry-through bulkheads. A concept sketch is shown in Figure 49, and system operation is outlined in Figure 50. The use of the bulkhead was for sizing purposes only and in no way limits the concept to similar shaped parts. Further, the concept is easily adaptable to addition of smaller cold working tools that can SWCW locations in planes not perpendicular to the main hydraulic mechanism.

System operation would begin with a part³ being loaded into the tool, with the X-Y table in a load/unload position. A carrier, or other mechanism sized to each different part to be processed, will position the part in place on the tool. The carrier may be separate from or integral with the tool. If separate, a means will have to be provided for positioning and securing the carrier onto the tool.

After loading and securing the part, the operator will initiate a cold working cycle using a rigorous means to identify the part type, and other part control numbers to the control system (RFID, barcode, etc.). Appropriate activity will be shown on a control panel display.

After ensuring that the control system has positively identified the specific part, cycle start will begin with an active operator input. The first action will be to locate the determinate assembly or reference feature on the part. Expected position will be known using information in pre-loaded part data tables. The part will move to the expected position and the laser measurement systems (or other system) will be used to locate the reference “0” position from which all areas to be cold worked can be located.

Cold working begins by movement of the X-Y table to the proper location for each hole. The Z-axis system may be used to move the part up or down to clear features as necessary. The tool changers will locate and load proper indenters, from information in the data tables, for the area to be cold worked.

³ Although the system is envisioned for near net shape parts, to maximize efficiency of cold working operations, there is no difference in operation for SWCW of a net shape part.

After moving the proper location, the Z-axis control system will activate to a neutral load position, to ensure compliance of the part during indenting. The indenting will follow to a prescribed load based on pre-determined tables. The depth of both the upper and lower dimples produced will be measured by a non-contact measurement system (e.g., laser). Should either dimple not be deep enough, the system will re-position itself, the load increased by a pre-determined algorithm, and the location re-processed. Learning systems will record and adjust the applied load for subsequent parts.

The system will then move the part for SWCW of the next location and the process repeated. After all locations are done and processing data recorded, the system moves to an unload position.

The automated SWCW tool is comprised of many elements that are commercial-off-the-shelf (COTS) components (X-Y positioning system, control system, hydraulic ram with internal displacement system, load cell, tool changers, laser measurement, etc) or are developed from conventional design practice (reaction frame). The single unique element, although built from COTS components, is the mechanism of the Z-axis compliance system during the indenting cycle.

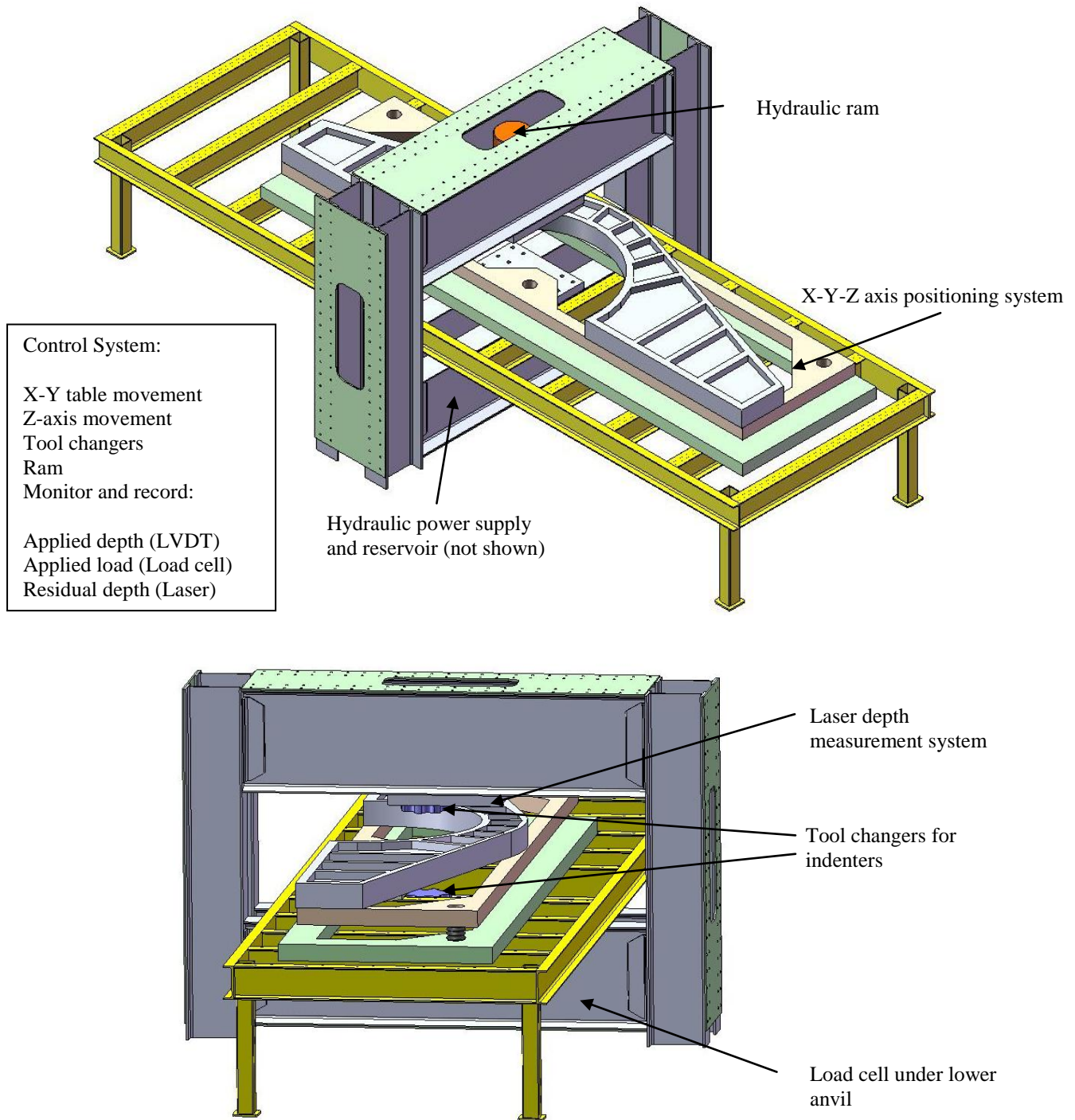


Figure 49. Concept Sketch – Automated SWCW Tool

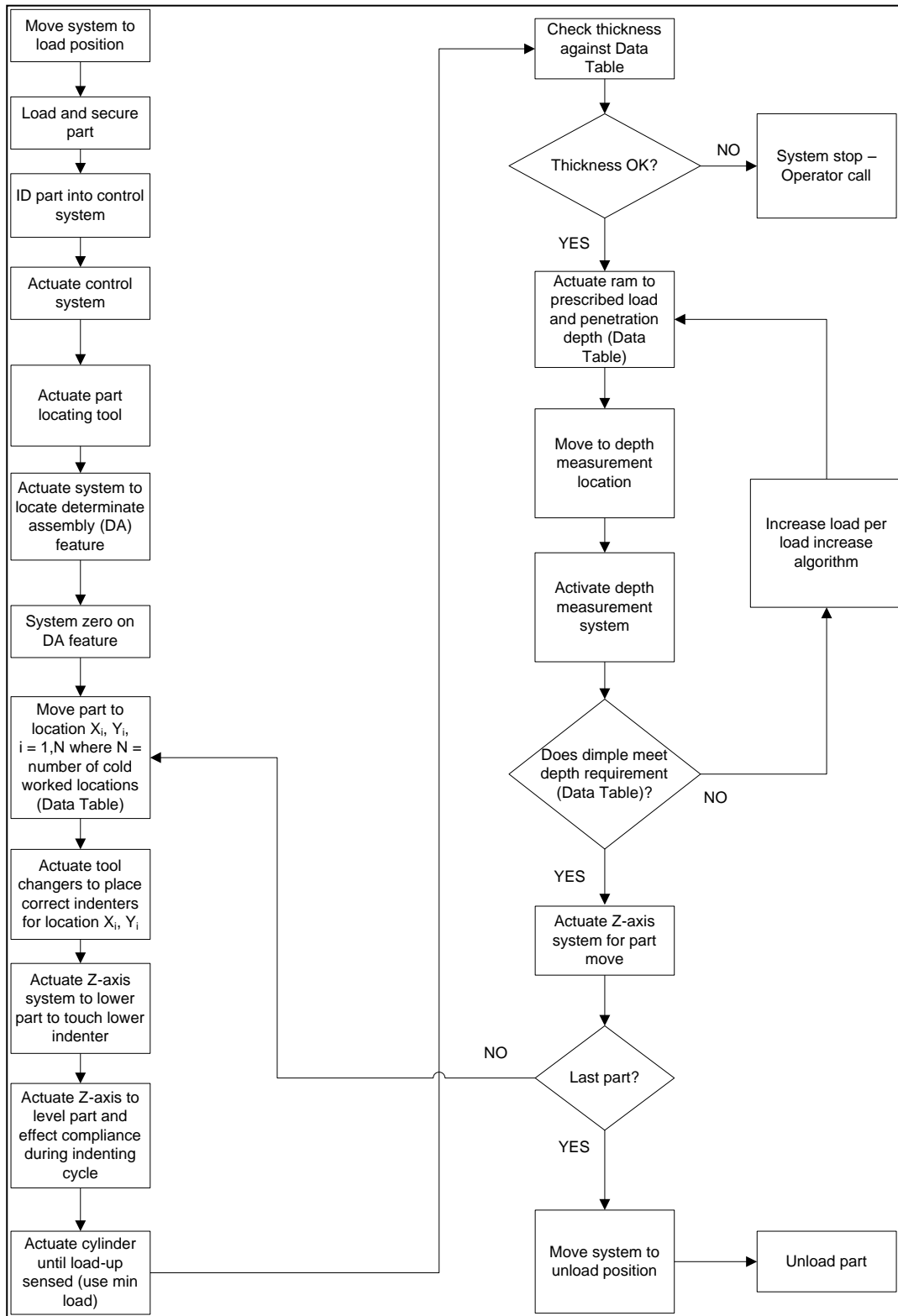


Figure 50. Process Control (Typical) – Automated SWCW Tool

Table 3. Control and Data Tables (Typical) – Automated SWCW Tool

CONTROL INPUT

Date/Time
Operator
P/N
S/N
Control Numbers A-x

DATA TABLE

P/N
Determinate Assembly (DA) hole location
Hole ID
X
Y
Thickness
Indenter
Initial load
Target applied depth
Load increase algorithm
Required residual depth

RECORD TABLE

Date	
Time	
P/N	
S/N	
Control Numbers A-x	
Each ram cycle, i	
Location	X, Y
Applied load	P_i
Residual Depth	D_i

The main element of the compliance system is a “spring table” that positions the part and holds it level in a horizontal plane, while simultaneously allowing the part to move vertically (Z-axis) during the indenting cycle. The compliance system accounts for varying thickness of locations to be SWCW’d, without the need for a second hydraulic ram. The design trade-off is self-evident; displacement or load control of two axially aligned opposing hydraulic cylinders is extraordinarily difficult while a compliance system is straight-forward. Nonetheless, current lab fixtures for SWCW do not simulate the dynamics of the compliance system so it was prudent to build a mock-up.

A fixture was designed and manufactured that simulates the compliance system and was proof-tested during the investigation (Figure 51). Later 1.125 inch SWCW specimens (Section 4.2) were processed successfully using this fixture.



Figure 51. Compliance System Mock-up with 1.125 inch Specimen

6. Conclusions

1. StressWave Cold Working (SWCW) provides a significant fatigue and crack growth life improvement in both 7085-T7651 plate and 7050-T7451 plate, for all the hole diameters, thicknesses, and specimen grain orientations tested.
2. SWCW, when performed on parts in a near net shape condition, provided fatigue life improvements ranging from 2.2 to over 47 times the life of the non-treated parts, for all the hole diameters, thicknesses, and specimen grain orientations tested..
3. In comparison, Split sleeve cold working provided fatigue life improvements ranging from 1.6 to over 4 times the life of the non-treated parts, for all the hole diameters, thicknesses, and specimen grain orientations tested.
4. SWCW, when performed on parts in a near net shape condition, provided fatigue life improvements greater than that provided by split sleeve cold working with improvements ranging from over 1.5 over 12 times, for all the hole diameters, thicknesses, and specimen grain orientations tested.
6. The formation of compressive residual stress states through SWCW were well characterized via a sophisticated finite element model and validated using X-ray and neutron diffraction measurements.
7. Tooling concepts were developed and are adaptable to automation using conventional tooling methods and processes for implementation.
8. Upstream SWCW is proven to be a viable, robust process, allowing flexibility in the manufacturing process, which allows fastener holes and/or penetration holes to be cold worked prior to machining.
9. High strength aluminum alloys (7085, 7050) showed no susceptibility to cracking during SWCW in the short transverse orientation, or any other grain orientation as compared to split sleeve cold working which has been shown to have a tendency to crack fastener holes in high strength aluminum alloys during cold working.
10. Quality control, consisting solely of dimple depth measurements, has been shown to be reliable and consistent.
11. Optimization using “Response Surface Methodology” in a multi-level arrangement has been proven to be a rapid and effective means of development of tooling and process parameters.
12. OEM cost analysis of SWCW showed a potential 50% reduction in costs of cold working over the life of a jet fighter production program for a targeted F-35 bulkhead application that was selected for this program.

13. SWCW has been shown to be an environmentally benign cold working method as compared to split sleeve cold working, as there are no single use tooling, wear-out items (e.g., extra cutting tools), nor lubricants to dispose.

14. SWCW has no expendable or disposable tooling to purchase, receive, handle, inventory, retrieve, or disposal issues.

7. Recommendations

1. Continue proof-of-concept tooling development with tools closely aligned with actual production parts.
2. Establish partnership with OEM for demonstration of SWCW on a full-scale part and subsequent testing.
3. Conduct fatigue crack growth (FCG) testing under spectrum loading conditions on both SWCW & Split Sleeve cold working specimens on 7085-T7452 forging material. FCG tests should be done on “as-received” specimens and after elevated temperature exposure to determine the effects of temperature on the compressive residual stresses generated during cold working.

8. References

1. Easterbrook, Eric E., Nam, Taeksun, Landy, Michael, "Fatigue Life Enhancement of Fastener Holes Manufactured from High-Strength Aluminum Alloys," SBIR Phase I Final Report, Dec 2004, AFRL Contract FA8650-04-M-5607.
2. Boni, L., Lanciotti, A., Polese, C., "Fatigue and Crack Propagation in Open Hole Specimens with Cold Worked Holes," Department of Aerospace Engineering, University of Pisa, Pisa, Italy International Committee on Aeronautical Fatigue (ICAF) Conference, Pisa, Italy, 2007.
3. Duchet, M., Rossillon, F., Galtier, A., Landy, M., Easterbrook, E., "Improvement of Fatigue Strength of Spot Welds Using StressWave Technique," Welding in the World, Vol. 52, no. 1/2, 2008.
4. Kim, Dae-Wook, Allen, Phil, Nam, Taeksun, Shin, Hyeon-Jae, "Effect of Cold Working on Exit Burr Formation in Drilling," Transactions of NAMRI/SME, Volume 34, pp. 317-324, 2006.
5. Tan, Jeffrey M.L., Fitzpatrick, Mike E., and Edwards, Lyndon, "Fatigue Crack Growth at Stresswave Cold Worked Holes," Structural Integrity Group, Department of Materials Engineering, The Open University, Milton Keynes, UK, 2005.
6. Lim, B., Ryu, S., Blake, D., Kim, D., "Improvement of Fatigue Strength in Al Alloy Spot-welds by Cold Working," 13th International Pacific Conference on Automotive Engineering (IPC-13), Gyeongju, Korea, August 2005.
7. Kim, D., Spitsen R., Khosla, T., Li, W., Ryu, S., Lim, B., "A Study on Cold Working of Aluminum Spot Welds to Improve Fatigue Strength," Transactions of NAMRI/SME, Vol. 33, pp.251-258, May 2005.
8. Blake, D., Spitsen, R., Kim, D., Flinn, B. D., Ramulu, M., "Weld Quality Effects on Fatigue Enhancement of Resistance Spot Welds," Proceedings of 2005 Society of Experimental Mechanics Annual Conference & Exposition, Portland, OR, June 2005.
9. Flinn, B. D., Spitsen R., Kim, D., Nam, T., Easterbrook, E., "Fatigue Strength Improvement of Low Carbon Steel Resistance Spot Welds by the StressWaveTM Process," SAE Paper Number 2005-01-903, SAE World Congress, April 2005.
10. Spitsen, R., Kim, D., Flinn, B., Ramulu, M., Easterbrook, E. T., "The effects of post-weld cold working processes on the fatigue strength of low carbon steel resistance spot welds," Proceedings of 2004 ASME International Mechanical Engineering Congress & Exposition, November 13-19, 2004, Anaheim, California.
11. Flinn, B. D., Wiegman, M. E., Landy, M., Nam, T., Easterbrook, E., StressWave Fatigue Life Improvement Process," SAE Technical Paper #2004-01-0630, SAE World Congress, 2004.

12. Dietrich, G. and Potter, J. M., "Stress Measurements on Cold-Worked Fastener Holes", *Advances in X-Ray Analysis*, Vol. 20. 1977.
13. MIL-HDBK-5G, "Metallic Materials and Elements for Aerospace Vehicle Structures," United States Air Force.
14. FTI Engineering Process Specification FTI8101C, "Cold Expansion of Fastener and Other Holes Using the Split Sleeve System (CX) and Countersink Cold Expansion Nosecap (CCX)," Fatigue Technology, Inc., 1994.
15. "Special Coldworking Process for Non-Fastener Holes in Aircraft Structures," Lockheed Martin LMA-PA020C, October 2006, Lockheed Martin Aeronautics Corporation.

LIST OF ACRONYMS, ABBREVIATIONS, AND SYMBOLS

ACRONYM	DESCRIPTION
2D	Two Dimensional
3D	Three Dimensional
AFRL	Air Force Research Laboratory
COTS	Commercial Off-the-Shelf
FE	Finite Element
Hz	Hertz
In	Inches
KSI	1000 pounds per square inch
L	Longitudinal Grain Orientation
LIF	Life Improvement Factor
LMAC	Lockheed Martin Aeronautics Company
LS-DYNA	Livermore Software Technology Company's Post-Yield Finite Element Software
LS-OPT	Livermore Software Technology Company's Post-Yield Finite Element Optimization Software
LT	Longitudinal-Transverse Grain Orientation
LVDT	Linear Variable Displacement Transducer
NF	No Failure
NIST	National Institute of Standards and Technology
PF	Pressure Foot
PSI	Pounds per square inch
PSIG	Pounds per square inch gauge
R	Stress/Load Ratio
RFID	Radio Frequency Identification Device
SBIR	Small Business Innovative Research
SWCW	StressWave Cold Working
ST	Short-Transverse Grain Orientation
STDN	Standard Tool Diameter Number
SW	StressWave, Inc.
USAF	United States Air Force
USCW	Upstream Cold Working